Wiley Online Library

ChemBioEng Reviews

Risk Identification and Safety Technology for Hydrogen Production from Natural Gas Reforming

Lele Feng[1], Yifan Gu[2], Jiabao Pang[2], Liangliang Jiang[3],*, Jie Liu[2,4], Hang Zhou[5],*, Biao Wang[6], Saeideh Babaee[7]

Abstract

The hydrogen production from natural gas has advantages of low investment, low carbon emission, and high hydrogen production rate. This paper briefly describes the technical overview of hydrogen production from natural gas reforming and identifies its risk factors. According to the dangerous characteristics of high reaction temperature, easy leakage of reaction medium, flammability, and explosion in the process, the intrinsic safety of the process is discussed in combination with relevant research and industrial experience. The safety requirements of key equipment and materials are introduced in detail, followed by the optimization methods of process safety that can be taken in the engineering process. Besides, the accident prevention measures for emergency shutdown and fire explosion are summarized. Finally, the future research demands are put forward from the perspective of research and development, which is instructive for the safe hydrogen production from natural gas in the future.

Keywords: Hydrogen production, Methane reforming, Natural gas reforming, Process safety optimization, Risk factors

Received: July 13, 2023; *revised:* November 08, 2023; *accepted:* January 15, 2024

DOI: 10.1002/cben.202300049

1 Introduction

The energy crisis, environmental pollution, and global warming have become urgent challenges shared by all mankind in the 21st century [1–3]. Hydrogen energy is a kind of clean energy, which has the advantages of high energy density and no pollution during utilization [4, 5]. It is considered an attractive solution to address three urgent challenges and will occupy an important position in the future energy pattern [6, 7].

Hydrogen production, as the primary link in the entire hydrogen industry chain, has been highly valued by the major economies around the world, including the United States, the European Union, China, and Japan [8–11]. In the existing hydrogen production technologies, coal-based hydrogen production has high carbon emissions, while methods such as electrolytic water hydrogen production, photolysis water hydrogen production, and biomass hydrogen production have low technological maturity and high production costs, making it difficult to achieve large-scale promotion and application in the short term [12–15].

Blue hydrogen production from natural gas (NG), which meets both the carbon footprint and competitive cost requirements, will be the preferred large-scale hydrogen production technology during the energy transition (Fig. 1) [16–18]. Notably, the global NG supply chain and the improvement of NG infrastructure in various countries have further contributed to the booming NG-to-hydrogen industry [19–21]. Along with the growth in penetration rate of carbon capture and utilization (CCU) technologies, the NG-to-hydrogen industry is poised to play a more positive role in carbon-neutrality plans [22, 23].

[1] Dr. Lele Feng https://orcid.org/0000-0001-5090-5295
Jiangsu Key Laboratory of Coal-based Greenhouse Gas Control and Utilization, China University of Mining and Technology, 221008 Xuzhou, Jiangsu, China.

[2] Yifan Gu, Jiabao Pang, Jie Liu
School of Safety Engineering, China University of Mining and Technology, Xuzhou, 221116, China.

[3] Dr. Liangliang Jiang (jial@ucalgary.ca)
Department of Chemical and Petroleum Engineering, The University of Calgary, Calgary, Alberta, Canada.

[4] Jie Liu
Department of Energy and Power Engineering, Tsinghua University, Beijing, 100084, China.

[5] Dr. Hang Zhou (18811709095@163.com)
Department of Chemical Engineering, University of Utah, Utah, 84108, U.S.A.

[6] Biao Wang
Key Laboratory of Hubei Province for Coal Conversion and New Carbon Materials, Wuhan University of Science and Technology, Wuhan, 430081, China.

[7] Dr. Saeideh Babaee
Department of Civil and Environmental Engineering, University of the Witwatersrand, Wits, 2050, South Africa.

 © 2024 Wiley-VCH GmbH

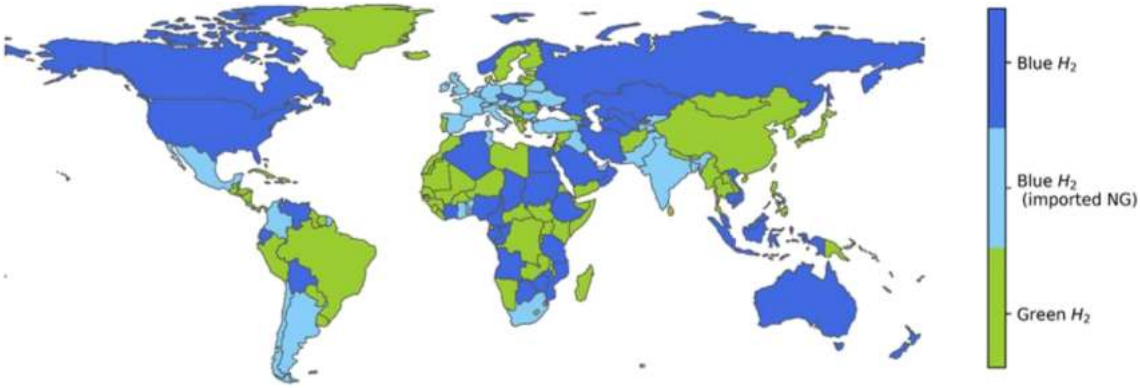

Figure 1. Countries colored by least marginal cost H_2 technology based on 2020 regional wholesale natural gas prices and 35 $/MWh cost of renewable energy assumption for green H_2 production (~ 2 $/kg of H_2) [16].

However, due to the complexity of the process system, multiple key equipment components, high material requirements, and the flammable and explosive characteristics of the main reactants and products in the hydrogen production from NG, there are accident hazards in all steps of the process [24]. In particular, hydrogen, as the main reaction medium, has the characteristics of low ignition energy [25], wide explosion limit range (4–75 %) [26], fast flame propagation velocity [27], and high diffusion coefficient [28], posing a significant safety threat. Public acceptance affects the development of the hydrogen economy, which requires that the probability and consequence severity of potential accidents at hydrogen production plants and ancillary infrastructure be maintained at tolerable levels in the long term [29].

Few comprehensive and systematic research is reported on the safety problem of the hydrogen production from NG, which limits the development of its industrial application. Herein, the hazardous factors in the process of hydrogen production from NG are identified and summarized. Then, combined with relevant research, the material safety requirements for the key equipment are analyzed. Safety optimization suggestions are proposed for the different stages in the whole process. The accident prevention and control measures for emergency shutdown and fire explosion are described. Finally, research demands are proposed from the perspectives of both basic research and technology, providing reference for the safe development of hydrogen production from NG.

2 Foundational Researches on Hydrogen Safety Modeling

The various devices that make up the hydrogen production line are interconnected and complicate with each other, which is a complex and uncertain risk system. Due to the interdependence of various devices and the hazardous nature of hydrogen, the initial minor accident may evolve into a chain event (i.e., domino effect) and ultimately suffer catastrophic losses [30]. The spread of accidents requires the release of escalation vectors from uncontrolled units. The probability of accident escalation is influenced by factors such as material type, vector direction, distance, and device vulnerability [31]. In order to minimize potential losses, various risk models have been continuously proposed and improved.

In early risk assessment efforts for hydrogen facilities, hazard and operability (HAZOP) and failure mode and effects analysis (FMEA) were used for hazard identification, event tree analysis (ETA) was used to describe accident scenarios, and fault tree analysis (FTA) was applied to deduce uncertainty propagation paths [32–34]. Moonis et al. [33] conducted a semi-quantitative risk assessment of hydrogen storage and transportation infrastructure through HAZID brainstorming and a risk matrix model. Mohammadfam and Zarei [34] presented an analytical framework for reviewing societal risks in hydrogen plants, including both, a qualitative part: HAZOP and preliminary risk analysis (PRA), and a quantitative part: ETA and risk and consequence simulator. However, the applicability of these traditional approaches is limited by their own static structure, uncertainty in the input and output data, and the inability to model conditional dependencies.

The Bayesian network (BN) is a directed acyclic graph used for inference in uncertain scenarios [35]. Each node represents a random variable. Given the conditional dependency relationship between random variables, the joint probability distribution $P(v)$ of a set of variables can be calculated according to Eq. (1). The dynamic Bayesian network (DBN) is an extension of the BN, which can help to explicitly modeling the evolution of a set of random variables on discrete time lines [36, 37]. According to Eq. (2), the joint probability distribution of a set of random variables on the timeline can be calculated.

$$P(v) = P(X_1, X_2, \ldots X_n) = \prod_{i=1}^{n} P(X_i | pa(X_i)) \tag{1}$$

$$P\left(v^{t+\Delta t}\right) = P\left(X_1^{t+\Delta t}, X_2^{t+\Delta t}, \ldots X_n^{t+\Delta t}\right) = \prod_{i=1}^{n} P\left(X_i^{t+\Delta t} \middle| X_i^{t}, pa\left(X_i^{t}\right), pa\left(X_I^{t+\Delta t}\right)\right) \tag{2}$$

In recent years, they have been widely used for analyzing the safety risks and vulnerabilities of a chemical production line, which to some extent breaks through the limitations of traditional approaches. Adedigba et al. [38] proposed a BN-based process risk model, thus establishing the link between process

© 2024 Wiley-VCH GmbH

21969744, 0, Downloaded from https://onlinelibrary.wiley.com/doi/10.1002/cben.202300049 by China University Of Mining, Wiley Online Library on [31/01/2024]. See the Terms and Conditions (https://onlinelibrary.wiley.com/terms-and-conditions) on Wiley Online Library for rules of use; OA articles are governed by the applicable Creative Commons License

21969744, 0, Downloaded from https://onlinelibrary.wiley.com/doi/10.1002/cben.202300049 by China University Of Mining, Wiley Online Library on [31/01/2024]. See the Terms and Conditions (https://onlinelibrary.wiley.com/terms-and-conditions) on Wiley Online Library for rules of use; OA articles are governed by the applicable Creative Commons License

deviations and potential loss prediction. Guo et al. [39] used fuzzy set theory (FST) for DBN modeling to enable quantification of the propagation of uncertainty over time. Zarei et al. [40] incorporated the D number theory (DNT) and best-worst method (BWM) into DBN for dealing with risk assessment under epistemic uncertainty.

Amin et al. [41] developed an integrated BN-based safety and security analysis framework that considers both physical and cyber attacks on production facilities. Huang et al. [42] proposed a quantitative vulnerability assessment method for chemical systems that greatly optimizes deployment for safety barriers. Ding et al. [43] innovatively used the fire synergistic effect model (FSEM) to study the spatiotemporal evolution of the domino effect and measured its risk with the energy accumulation effect.

3 Risk of Hydrogen Production from Natural Gas

3.1 Process Flow

There are three types of hydrogen production technologies using NG as the main raw material: steam methane reforming (SMR) [44], partial oxidation reaction (POX) [45], and autothermal reforming (ATR) [46]. Among them, SMR is the most mature and widely employed hydrogen production technology in industry [47]. The discussion in the following part of this article is focused on SMR, which mainly involves the NG pretreatment, methane reforming, purification of hydrogen, and other procedures, as illustrated in Fig. 2 [48, 49].

To meet the catalyst's limit on the sulfur content in the raw materials (< 0.1 ppm), it is necessary to desulfurize the raw gas (i.e., NG pretreatment), including two steps in fixed-bed reactors: hydrogenation and hydrogen sulfide removal. At a temperature of 400 °C and a pressure of 25 bar, the gas reacts with hydrogen to convert organic sulfur into inorganic sulfur (H_2S)

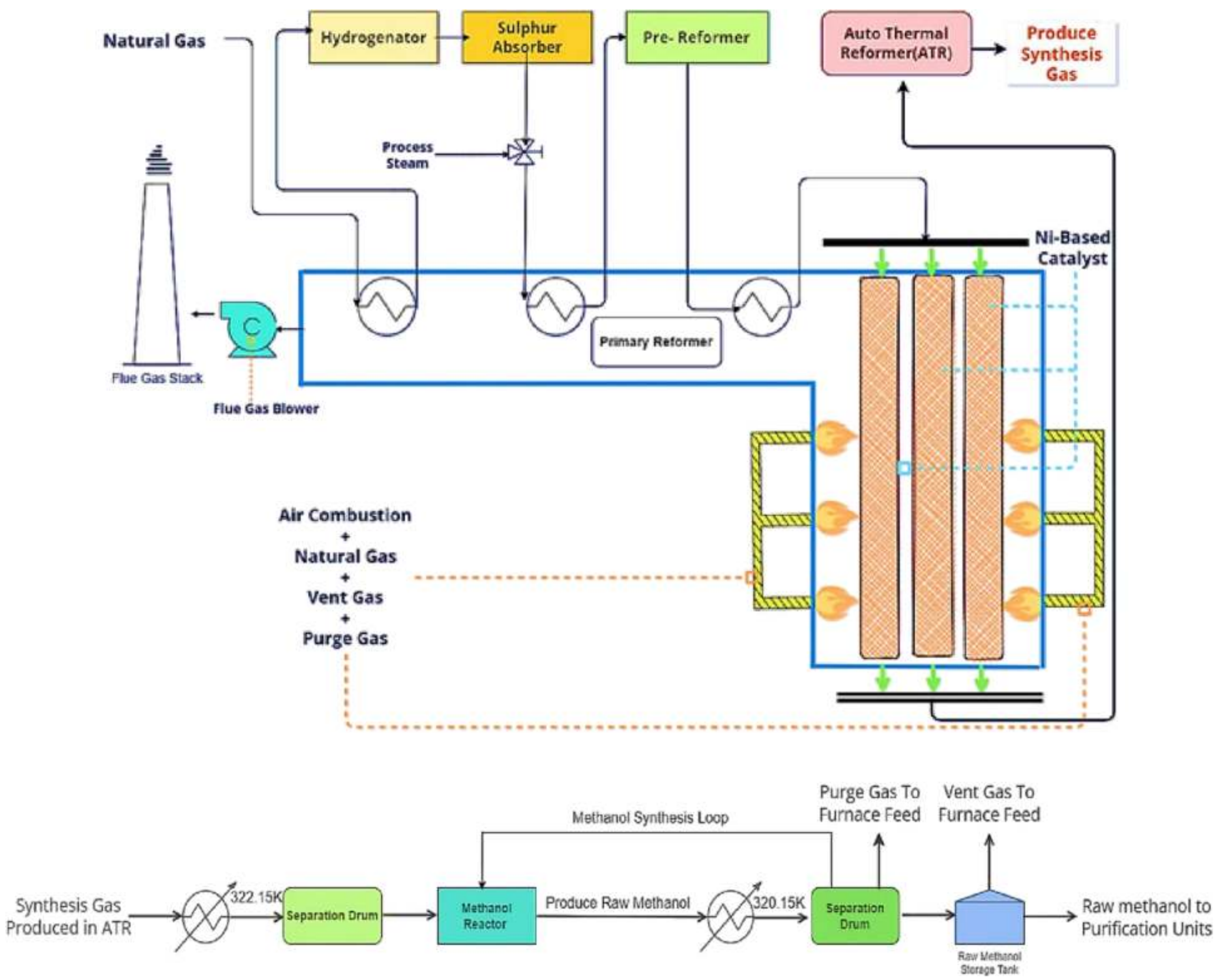

Figure 2. Process diagram for SMR hydrogen production [49].

with the help of cobalt molybdenum oxide, and H_2S is adsorbed using zinc oxide desulfurizer subsequently [50]. Next, the pretreated NG undergoes a strong endothermic reforming reaction (750 °C, 30 bar) with water vapor on the Ni/Al_2O_3 catalyst bed in the primary-reformer to generate synthesis gas (i.e., CO, H_2) [51]. Then, synthesis gas is regulated to 350 °C and 25 bar through a temperature- and pressure-reducing valve (TPRV) before entering the secondary-reformer. In the secondary-reformer, CO reacts with water vapor to produce more H_2 [52]. The gas temperature is cooled to 40 °C and finally enters the hydrogen purification unit, where impurities such as CH_4, CO, CO_2, and H_2O are removed. At present, pressure swing adsorption (PSA) units are mainly employed for purification.

3.2 Risk Factors

(1) Fire and explosion. The hydrogen production process from NG mainly involves three types of flammable and explosive gases: raw material CH_4, intermediate product CO, and target product H_2. Part of the physical and chemical parameters of them are given in Tab. 1. Due to the wide explosion limit range, low ignition energy, and easy leakage characteristics of H_2 [53], the high-temperature surface of the production equipment, electrical sparks during the hydrogen release, lightning, and human electrostatic sparks are all potential ignition sources.
(2) Toxic substances. There are many types of toxic substances present in the hydrogen production process. There are toxic substances such as H_2S in the desulfurization process, and toxic substances such as CO and hydroxyl nickel exist in the steam conversion process [54]. Once gas leakage occurs in either containers or pipelines, it will pose a risk of poisoning to inspection workers.
(3) High-temperature thermal radiation. The NG pretreatment and methane reforming steps are carried out under high-temperature conditions. The heating equipment and reaction vessel continuously generate thermal radiation to the external environment. In order to facilitate equipment heat dissipation, most of the heating furnaces and reaction towers are arranged in an outdoor environment. If there is no safety enclosure around them, it will cause high-temperature thermal radiation hazards to the on-site construction workers.
(4) Noise. There are many noise sources above 70 dB, such as centrifugal compressor, high-pressure differential throttle valve, high-pressure material delivery pump, and fan. The noise intensity generated by the compressor is the largest (90–105 dB).
(5) Dust. It mainly comes from the process of replacing catalysts. The insulation materials during pipeline maintenance can also generate a lot of dust.

The occupational health standards in different nations are summarized in Tab. 2.

4 Material Requirements for Safety

4.1 Reforming Furnace

The reforming furnace for hydrogen production is the core equipment that completes the steam reforming reaction, consisting of the refractory wall, reforming tubes, burners, etc. [55]. Its structure is displayed in Fig. 3. The reforming tube has the characteristics of both a reactor and a pressure vessel, and is a key component of the SMR reaction [56].

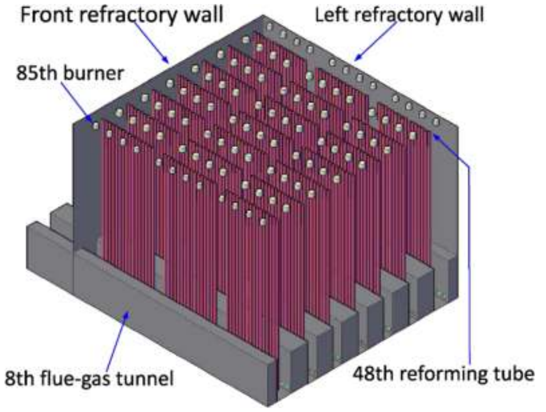

Figure 3. Isometric view of the reforming furnace in which the right and back refractory walls are made transparent to exhibit its interior components [57].

Due to the uneven temperature distribution in the reaction and the weld defects, it is easy to lead to local overheating of the tube, resulting in carbide deposition, microstructure coarsening, and microcracks, which gradually develop to irreversible creep damage and early failure or burst of the tube [58]. The resulting release of internal high-temperature and high-pressure reactants can lead to serious production accidents such as jet fires and explosions [59,60]. Thus, the

Table 1. Partial physical and chemical parameters of CH_4, CO, and H_2.

Hazardous substances	Relative density[a)]	Ignition temp.[b)] [°C]	Ignition point [°C]	Minimum ignition energy [mJ]	Explosion limit [V%]
CH_4	0.55	537	650–750	0.470	5.0–15.0
CO	0.97	610	641–658	0.233	12.5–74.2
H_2	0.07	500–571	580–600	0.017	4.1–75.0

[a)] Density of air is defined as 1; [b)] minimum temperature required for spontaneous combustion of a substance under the condition of no ignition source.

© 2024 Wiley-VCH GmbH

21969744, 0, Downloaded from https://onlinelibrary.wiley.com/doi/10.1002/cben.202300049 by China University Of Mining, Wiley Online Library on [31/01/2024]. See the Terms and Conditions (https://onlinelibrary.wiley.com/terms-and-conditions) on Wiley Online Library for rules of use; OA articles are governed by the applicable Creative Commons License

Table 2. Comparison of occupational health standards for toxic substances, high-temperature thermal radiation, noise, and dust in different nations.

Nation	United States	China	Japan	Germany	India
STEL[a)] of H_2S [ppm]	10	10	5	5	10
PEL[b)] of H_2S [ppm]	5	1.6	1	1	5
STEL of CO [ppm]	200	30	30	35	50
PEL of CO [ppm]	50	20	25	25	30
Relative humidity [%]	20–60	40–70	30–70	40–60	30–60
MRTL[c)] [$W\,m^{-2}$]	2.5	5	20	10	–
Maximum temperature limit [°C]	24	28	30	30	40
MPE[d)] of noise [dB]	140	137	132	135	140
4 h TWA[e)] sound level [dB]	88	87	87	88	87
2 h TWA sound level [dB]	91	90	90	91	90
1 h TWA sound level [dB]	94	93	93	94	93
STEL of inhalable dust [$mg\,m^{-3}$]	5	10	10	10	5
8 h TWA of inhalable dust [$mg\,m^{-3}$]	1	4	1	1	1
PEL of silica dust [$mg\,m^{-3}$]	0.05	0.15	0.3	0.15	0.3
8 h TWA of silica dust [$mg\,m^{-3}$]	0.05	0.1	0.1	0.1	0.1

[a)] Short-term exposure limit (15 min); [b)] permissible exposure limit; [c)] maximum recommended thermal load; [d)] maximum permissible exposure; [e)] time-weighted average.

reforming tube is usually made of chromium nickel alloy, developed from the initial HK40, Cr25Ni20, and Incoloy 800HT to the latest micro alloyed steel 22.5Cr25Ni1.5Mo-Nb-N and Cr25Ni35-Nb-Ti-Zr by centrifugal casting [61, 62]. With such tube made of micro alloys, the outlet temperature can reach up to 900 °C. The rise in reaction temperature increases the intensity of the conversion reaction, thereby reducing the proportion of remaining CH_4 in the conversion gas, reducing the water carbon ratio, thermal load of the conversion furnace, and fuel consumption, reducing the burden on downstream heat recovery equipment, and improving the long-term safe operation ability of the device.

In order to improve the insulation effect and reduce thermal radiation damage, the outer wall of the furnace should be made of low chromium molybdenum steel (e.g., 1.25Cr-0.5Mo, 9Cr-1Mo-V), and the inner lining of the furnace should be made of zirconium containing refractory bricks (e.g., ZS-1300, ZS-1500) or high-aluminum refractory bricks (e.g., DRL-155, DRL-150) [63, 64]. The comparison of some parameters between the special materials mentioned in this section and other ordinary materials is given in Tab. 3.

In addition, the application of magnetic sensors based on changes in magnetic flux density in the detection of carburization damage can provide early warning of reforming tube failure [65]. Its geometric structure is illustrated in Fig. 4.

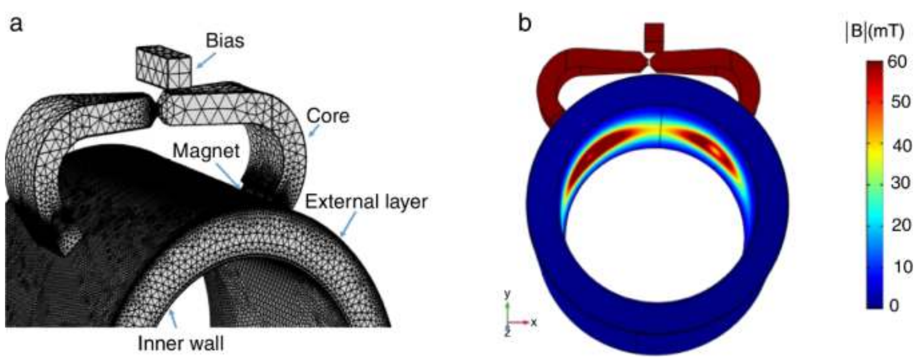

Figure 4. Magnetic sensor geometry. (a) Mesh in the model geometry, (b) magnetic flux density through-wall the carburized sample (closed magnetic circuit) [65].

4.2 Catalysts for SMR

Developing high-performance SMR reaction catalysts is an indispensable issue related to process safety [66]. SMR catalysts need to withstand the challenges of long-term stability and avoiding rapid deactivation due to sintering and coking [67]. Frequent replacement of failed catalysts means frequent interruptions and restarts of the reforming furnace, which shortens its life and amplifies the accident risk. Additionally, the deacti-

 © 2024 Wiley-VCH GmbH

21969744, 0, Downloaded from https://onlinelibrary.wiley.com/doi/10.1002/cben.202300049 by China University Of Mining, Wiley Online Library on [31/01/2024]. See the Terms and Conditions (https://onlinelibrary.wiley.com/terms-and-conditions) on Wiley Online Library for rules of use; OA articles are governed by the applicable Creative Commons License

Table 3. Comparison of parameters between materials used in the reforming furnace and other ordinary materials.

Material name	UNS No.	DEN[a) [$g\,cm^{-3}$]	YS[b) [MPa]	TS[C) [MPa]	TC[d) [$W\,m^{-1}K^{-1}$]	T_{max}[e) [°C]	CS[f) [MPa]	CTE[g) [$m^{-1}\,°C^{-1}$]	Price [$\$\,t^{-1}$]
20Cr25Ni20	S31008	7.98	205	515	15	1100	–	16.0×10^{-6}	2400
HK40	J94204	8.19	240	425	18	815	–	13.9×10^{-6}	2100
Incoloy 800HT	N08811	8.40	415	690	11.4	950	–	13.3×10^{-6}	2800
22.5Cr25Ni1.5Mo-Nb-N	N06059	9.07	379	827	11.2	1100	103	13.8×10^{-6}	3500
Cr25Ni35Nb-Ti-Zr	N06030	8.22	240	620	9.3	1050	103	13.9×10^{-6}	3380
9Cr-1Mo-V	K90941	7.85	415	585	35.6	650	–	11.5×10^{-6}	1350
1.25Cr-0.5Mo	K11872	7.84	310	515	31.9	550	–	12.8×10^{-6}	1200
HRB400*)	G10450	7.85	450	700	18.6	300	–	11.7×10^{-6}	570
0Cr18Ni9*)	S30400	7.93	205	515	16.3	550	–	17.2×10^{-6}	1300
S316*)	S31600	8.01	205	515	16.8	650	80	16.5×10^{-6}	1100
ZS-1300	–	5.45	200	400	2.5	1650	40	7.5×10^{-6}	960
ZS-1500	–	5.65	200	400	2.5	1700	45	6.5×10^{-6}	980
DRL-155	–	2.54	40	60	1.6	1520	35	6.5×10^{-6}	910
DRL-150	–	2.62	40	60	1.5	1550	37	6.0×10^{-6}	970

a) Density; b) yield strength; c) tensile strength; d) thermal conductivity; e) maximum service temperature; f) creep strength; g) coefficient of thermal expansion; *) conventional materials which are not suitable for assembling reforming furnace.

vation of the catalyst is accompanied by an increase in its thermal resistance, which may cause the outer tube wall temperature (OTWT) of the reforming tube to exceed the design limit value, leading to accelerated degradation of the microstructure of the tube wall and increasing the cracking risk [68]. Improving the carrier can enhance the stability of the catalyst.

Khosravani et al. [69] synthesized mesoporous γ-alumina via biotemplate method and prepared a Ni-Ce/Al_2O_3 catalyst using it as a supporting material. This biotemplated alumina forms a higher Brunauer-Emmett-Teller (BET) surface area under larger pore size compared with bulk one, so as to promote better dispersion of the active site. Therefore, less coke formation and better catalytic performance were observed in the SMR reaction using these mesoporous catalysts.

Adding various elements as promoters to Ni-based catalysts is also a major strategy to improve the long-term safety of the catalyst. For example, zirconium, yttrium, and lanthanum were found to be good texture promoters, which can increase the surface area of catalyst and dispersion of the active site [70]. The doping of Pd and Fe has been proven to enhance the anti-coking effect, and the Fe-promoted Ni catalyst is sulfur-resistant [71–73]. The doping of Re can enhance the stability of the overall catalyst by suppressing the oxidation of surface Ni atoms during the SMR [74]. Trace Ag addition (0.3 wt %) can significantly reduce carbon deposition of the catalyst [75]. The addition of Rh and Ir improves the catalyst's ability to resist Ni sintering [76]. Tab. 4 compares the performance of several different catalysts for SMR.

4.3 Pressure Swing Adsorption Device

Fig. 5 displays the configuration and running cycle schedules of a 16-bed PSA system. Due to frequent changes in internal pressure (fluctuating between 1 and 8 bar), metal fatigue, and long-term hydrogen embrittlement, the risk of sudden failure of PSA towers and their accessories is significantly increased [77]. In order to improve the reliability of the device and and minimize the risk of hydrogen leakage, it is recommended to use Ni-containing metal materials such as Austenitic stainless steel (e.g., S31603, S31608) with low hydrogen embrittlement sensitivity [78].

Tab. 5 compares the performance parameters between these metals and other ordinary metals. The hydrogen storage equipment in plants also has similar reliability requirements. The design of high-pressure gaseous hydrogen storage containers should focus on pressure risks, avoid overpressure explosions, and improve the charging and discharging of hydrogen storage tanks and the cycling stability of hydrogen. The development of liquid hydrogen storage requires the development of materials with good insulation and mechanical properties at low temperatures, which can reduce hydrogen embrittlement.

4.4 Programmed Control Valve

The PSA process is controlled sequentially, which involves the processes of adsorption, pressure equalization, sequential release, reverse release, and flushing in a step-by-step manner.

21969744, 0, Downloaded from https://onlinelibrary.wiley.com/doi/10.1002/cben.202300049 by China University Of Mining, Wiley Online Library on [31/01/2024]. See the Terms and Conditions (https://onlinelibrary.wiley.com/terms-and-conditions) on Wiley Online Library for rules of use; OA articles are governed by the applicable Creative Commons License

Table 4. Comparison of performance between different catalysts for SMR.

Catalysts	Support	Promoter	T [°C]	S/M[a]	GHSV[b] [mL g^{-1}h^{-1}]	CR[c] of CH_4 [%]
5.0%Ni	γ-Al_2O_3	–	700	3.0	24 000	90
13.0%Ni	γ-Al_2O_3	Ce	800	2.7	–	75
10.0%Ni	γ-Al_2O_3	–	700	2.5	6000	99
Ni	γ-Al_2O_3	Mg	850	1.2	60 000	60
19.9%Ni	γ-Al_2O_3	La–Ca	900	3.0	–	100
50.0%Ni	α-Al_2O_3	–	700	2.4	65 500	78
15.0%Ni	γ-Al_2O_3	Cu	700	4.0	–	95
10.0%Ni	α-Al_2O_3	$CaZrO_3$	700	1.0	60 000	67
5.0%Ni	γ-Al_2O_3	Ce–Zr	700	2.0	–	63
15.0%Ni	γ-Al_2O_3	–	700	–	18 000	99

[a] Ratio of steam/methane; [b] gas hourly space velocity; [c] conversion rate.

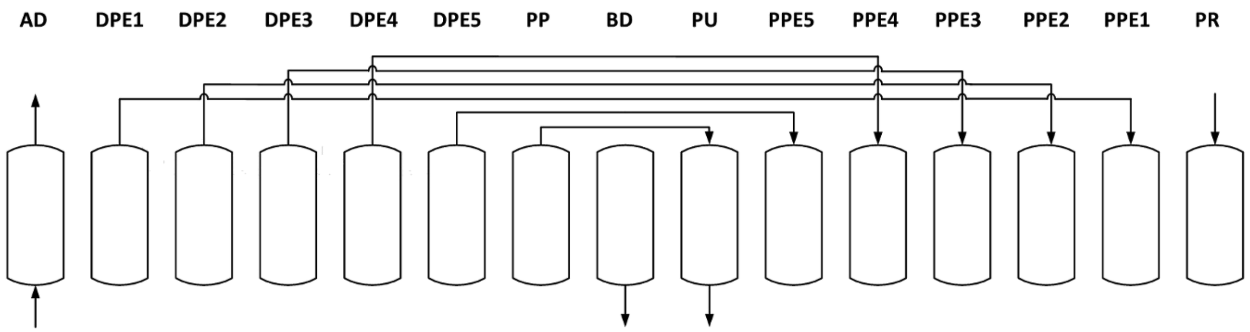

BED	STEP																															
1	AD								DPE1	DPE2	DPE3	DPE4	DPE5	PP						BD	PU						PPE5	PPE4	PPE3	PPE2	PPE1	PR
2	PPE1	PR	AD								DPE1	DPE2	DPE3	DPE4	DPE5	PP						BD	PU						PPE5	PPE4	PPE3	PPE2
3	PPE3	PPE2	PPE1	PR	AD								DPE1	DPE2	DPE3	DPE4	DPE5	PP						BD	PU						PPE5	PPE4
4	PPE5	PPE4	PPE3	PPE2	PPE1	PR	AD								DPE1	DPE2	DPE3	DPE4	DPE5	PP						BD	PU					
5	PU		PPE5	PPE4	PPE3	PPE2	PPE1	PR	AD								DPE1	DPE2	DPE3	DPE4	DPE5	PP						BD	PU			
6	PU				PPE5	PPE4	PPE3	PPE2	PPE1	PR	AD								DPE1	DPE2	DPE3	DPE4	DPE5	PP						BD	PU	
7	PU						PPE5	PPE4	PPE3	PPE2	PPE1	PR	AD								DPE1	DPE2	DPE3	DPE4	DPE5	PP						BD
8	PP	BD	PU						PPE5	PPE4	PPE3	PPE2	PPE1	PR	AD								DPE1	DPE2	DPE3	DPE4	DPE5	PP				
9	PP			BD	PU						PPE5	PPE4	PPE3	PPE2	PPE1	PR	AD								DPE1	DPE2	DPE3	DPE4	DPE5	PP		
10	PP					BD	PU						PPE5	PPE4	PPE3	PPE2	PPE1	PR	AD								DPE1	DPE2	DPE3	DPE4	DPE5	PP
11	DPE5	PP						BD	PU						PPE5	PPE4	PPE3	PPE2	PPE1	PR	AD								DPE1	DPE2	DPE3	DPE4
12	DPE3	DPE4	DPE5	PP						BD	PU						PPE5	PPE4	PPE3	PPE2	PPE1	PR	AD								DPE1	DPE2
13	DPE1	DPE2	DPE3	DPE4	DPE5	PP						BD	PU						PPE5	PPE4	PPE3	PPE2	PPE1	PR	AD							
14	AD		DPE1	DPE2	DPE3	DPE4	DPE5	PP						BD	PU						PPE5	PPE4	PPE3	PPE2	PPE1	PR	AD					
15	AD				DPE1	DPE2	DPE3	DPE4	DPE5	PP						BD	PU						PPE5	PPE4	PPE3	PPE2	PPE1	PR	AD			
16	AD						DPE1	DPE2	DPE3	DPE4	DPE5	PP						BD	PU						PPE5	PPE4	PPE3	PPE2	PPE1	PR	AD	

Figure 5. Step configuration of a 16-bed H_2 PSA cycle with five pressure equalisations, four adsorbing beds, and three purging beds (AD: adsorption, DPE: depressurizing pressure equalization, ID: idle, PP: providing purge, BD: blowdown, PU: purge, PPE: pressurising pressure equalization, PR: pressurization); $t_{AD} = t_{cycle}/4$; $t_{PP} = t_{PU} = 3t_{cycle}/16$; $t_{BD} = t_{DPE} = t_{PPE} = t_{PR} = t_{cycle}/32$) [79].

© 2024 Wiley-VCH GmbH

21969744, 0, Downloaded from https://onlinelibrary.wiley.com/doi/10.1002/cben.202300049 by China University Of Mining, Wiley Online Library on [31/01/2024]. See the Terms and Conditions (https://onlinelibrary.wiley.com/terms-and-conditions) on Wiley Online Library for rules of use; OA articles are governed by the applicable Creative Commons License

Table 5. Comparison of parameters between metals used in PSA devices and other ordinary metals.

UNS No.	DEN[a)] [g cm^{-3}]	YS [MPa]	TS [MPa]	El[a)] [%]	Ra[b)] [%]	HB[c)] [N mm^{-2}]	T_{max} [°C]
S31603	7.99	175	485	30	40	85–95	925
S31608	7.98	205	520	40	50	85–95	925
S30408	7.93	240	505	25	35	75–90	750
S31600	8.01	205	515	30	40	85–95	650
A96061	2.71	140	310	12	20	45–65	200
G10100	7.87	345	380	30	40	70–80	425

[a)] Elongation; [b)] reduction of area; [c)] Brinell hardness.

The step-by-step implementation of different programs relies on the on-off action of the programmable valve at a preset time. Therefore, during the completion of a process cycle, the programmable valve needs to be frequently started and stopped [80, 81]. Under alternating pressure and hydrogen environment, the valve stem is prone to fatigue failure, so the operational requirements and performance need to be higher than general valves. In particular, the working life of different caliber program control valves at the inlet and outlet of the PSA device's raw gas varies. Large caliber program control valves have a larger volume compared to smaller caliber program control valves, so they are subjected to higher stress loads during the startup and shutdown process and are more susceptible to damage. A large number of tests and data comparison of material characteristics show that 17-4PH martensite precipitation hardening stainless steel is suitable to replace 40Cr alloy steel as the stem material of large diameter program control valves with higher compressive strength and fatigue resistance [82, 83], so as to ensure the smooth completion of PSA and the safety and reliability of the system.

5 Process Optimization for Safety

5.1 Startup and Shutdown

During the start-up and shutdown of the device, the PSA device cannot provide sufficient desorbed gas as fuel for the burner of the converter, and NG must be introduced as supplementary fuel. Due to the difference in the calorific value between NG and the desorbed gas, the amount of NG required to maintain the same load is only one-third of that of the desorbed gas. Therefore, the existing burner nozzle opening rate is not suitable for NG working conditions, the flow and pressure during combustion cannot meet the requirements, and there is even a risk of backfire and explosion.

Research has found that it is difficult to burn safely when only NG is available. A report proposes a transformation method for the burner structure to achieve independent combustion of desorbed gas and NG. The burner is changed to an inner and outer casing structure, with the outer and inner casing conveying desorbed gas and NG, respectively, and holes are opened according to the corresponding opening rate. This structural modification avoids unstable combustion phenomena caused by different combustion heats and opening rates during the single combustion process, which is conducive to the safe operation of the conversion furnace.

5.2 Installation of Temperature- and Pressure-Reducing Valves

The reaction medium needs to be reduced in temperature and pressure by a TPRV during the transfer from primary-reformer to secondary-reformer and from secondary-reformer to the purification unit. The structure of the TPRV is illustrated in Fig. 6 [84]. Currently, many TPRVs are directly connected to

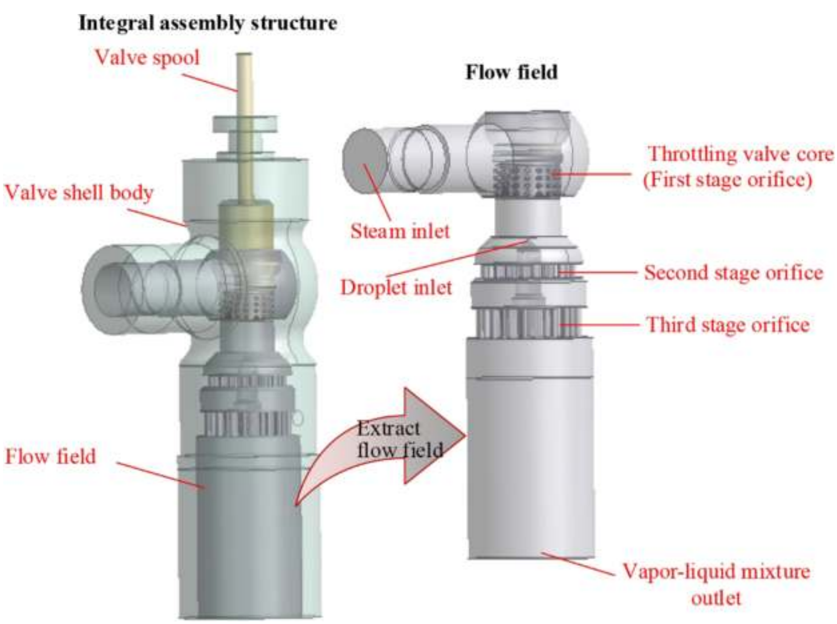

Figure 6. Structure of the TPRV [84].

21969744, 0, Downloaded from https://onlinelibrary.wiley.com/doi/10.1002/cben.202300049 by China University Of Mining, Wiley Online Library on [31/01/2024]. See the Terms and Conditions (https://onlinelibrary.wiley.com/terms-and-conditions) on Wiley Online Library for rules of use; OA articles are governed by the applicable Creative Commons License

process pipelines. This design and installation process are simple and direct. However, in actual industrial production, the high wall temperature and mechanical vibration of the process pipeline are directly transmitted to the control system of the TPRV through the connecting pipeline, which has adverse effects on the stable operation of the controller. Moreover, this connection structure is not convenient for the maintenance and repair of the TPRV, and it requires an overall shutdown for proceeding.

Research has shown that installing the process pipeline and the TPRV control system independently and connecting the subsequent components of the control valve with flanges or welding can greatly improve system reliability. Under this structural design, the control system is protected from the high temperature impact of the process pipeline. When the control system malfunctions, temporary adjustments are made using auxiliary lines, and maintenance of the control system can be completed without stopping operations. This type of connection between equipment is also applicable to other chemical production lines. It reduces the uncertainty of hazards due to mechanical vibration and heat transfer and facilitates temporary individual equipment maintenance.

5.3 Pressure Swing Adsorption Control

In actual industrial production, even if the PSA device operates at its optimal state, there are inevitably related disturbances, such as a sudden increase or decrease in feed volume at a certain time point. If not adjusted in advance, it will take a long time to restore the set value or even directly deviate from the operational requirements of the process, posing a threat to the safe operation of the device. Combining fuzzy control with existing Proportional Integral Derivative (PID) control can achieve real-time monitoring and intelligent control of the PSA process, thereby improving the stability of device operation. Martins et al. [85] developed a robust stabilization model predictive control (MPC) of PSA based on multi model uncertainty description to systematically adapt to typical cyclic steady state and various disturbances in the PSA process. Fig. 7 depicts the closed-loop behavior of PSA-controlled variables under the action of the controller.

5.4 Pd-Based Membrane Separation

Due to the infinite hydrogen permeation selectivity of dense Pd-based membranes compared to other gases, these membranes can replace PSA as the purification unit for SMR hydrogen production [86, 87]. Compared with traditional PSA, Pd-based membrane separation does not require frequent changes in device pressure and has significant advantages in safety, energy consumption, and process stability. Nevertheless, the commercial application of Pd-based membranes is limited by: (i) the high price of Pd, (ii) degradation mechanism of H_2-saturated Pd membranes susceptible to stress cracking after repeated temperature fluctuations, and (iii) the irreversible poisoning of Pd-based membranes by H_2S [88, 89]. Alloying with other metals can alleviate the first two defects of Pd-based membranes to a certain extent. For instance, Sanz-Villanueva et al. [90] prepared TiO_2/Pd membranes using raw TiO_2 particles as intermediate layers. This design greatly saves Pd usage. The membrane showed good mechanical stability for 200 h and complete selectivity for 1000 h at 400 °C. For the third defect, recent studies have found a positive effect of the applied electric field in preventing H_2S poisoning of the Pd membranes [91].

Moreover, with the improved performance of Pd-based membranes and SMR catalysts, simultaneous SMR reaction and in-situ hydrogen separation in membrane-integrated reformer reactors (MRRs) became possible. This MRR, with its compact structure and small floor area, provides an ideal

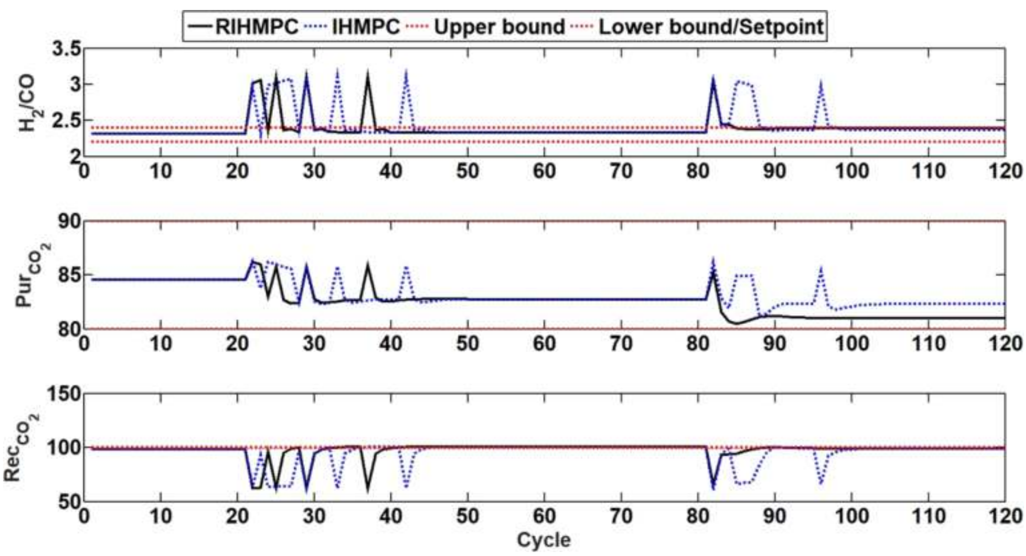

Figure 7. Closed-loop behavior of the controlled variables under RIHMPC and IHMPC controllers applied to the PSA unit [85].

© 2024 Wiley-VCH GmbH

21969744, 0, Downloaded from https://onlinelibrary.wiley.com/doi/10.1002/cben.202300049 by China University Of Mining, Wiley Online Library on [31/01/2024]. See the Terms and Conditions (https://onlinelibrary.wiley.com/terms-and-conditions) on Wiley Online Library for rules of use; OA articles are governed by the applicable Creative Commons License

choice for building urban hydrogen refueling stations based on the distributed production technologies. The scheme of an MRR is shown in Fig. 8. It is worth noting that, during the reaction process, H_2 continuously migrates from the reaction zone to the permeation zone, promoting the reaction to proceed forward. Thus, the temperature and pressure of SMR reaction in the MRR can be appropriately reduced to improve safety [92]. Ilianelli et al. [93] achieved a methane conversion rate of 50 % in a dense Pd-Ag MRR packed with a Ni-based catalyst under conditions of 450 °C and 3 bar, which is more than eight times that of a traditional SMR reactor under the same conditions.

5.5 Low-Load Operation

During peak NG usage, the device operates at low load, which can easily cause damage to the raw material compressor and converter furnace tubes, as well as catalyst carbon deposition, and cannot ensure long-term safe operation. In response to this issue, researchers have found through Aspen Plus software simulation and device operation verification that a smaller secondary line control valve can be set for the NG inlet control valve to increase control accuracy, reduce feed fluctuations, and meet the needs of low load NG inlet. By increasing the water carbon ratio of the SMR reaction, the outlet temperature and methane concentration of the converter are reduced, avoiding medium coking and the occurrence of red tubes and flower spots in the furnace tubes.

Tran et al. [57, 95] combined the furnace-balancing framework, the statistical-based model for the OTWT distribution, the valve-to-flow rate converter, and heuristic search algorithm to design a real-time SMR furnace balancing procedure (Fig. 9) to cope with such unexpected disturbances and ensure the safety of the device. The application of furnace temperature balancing technology can be extended to other chemical production processes to reduce the risk of uncertainty arising from an uneven temperature field distribution in the reaction vessel and to avoid premature failure of equipment components.

6 Emergency Response to Accidents

6.1 Emergency Shutdown

An emergency shutdown device (ESD), also known as safety instrumented system (SIS), is a safety protection system designed based on HAZOP and protection layer analysis results for industrial processes. It can automatically monitor the operating status of hydrogen production from the NG process. When the hydrogen production device needs to stop due to abnormal process parameters or sudden situations such as gas and power outages, the SIS system can detect and execute shutdown procedures in a timely manner, ensuring that the process is always in a safe state, thereby avoiding personal injury and economic losses [96].

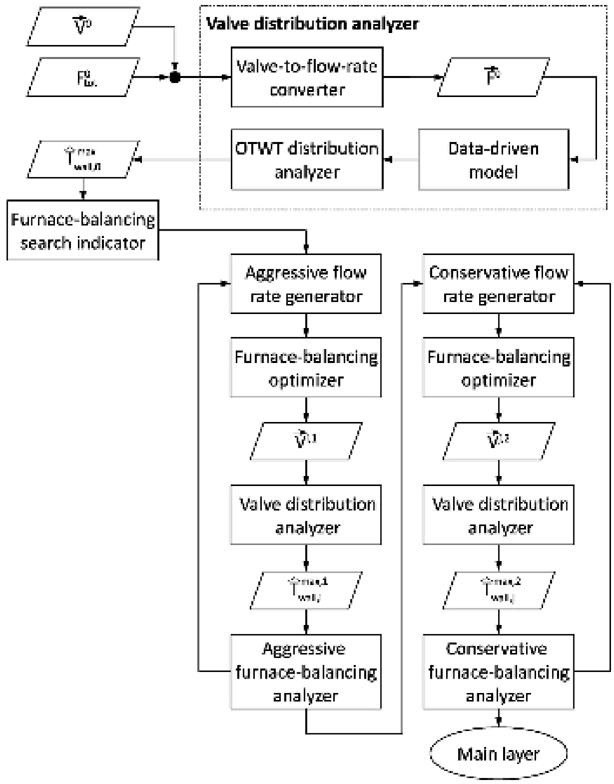

Figure 9. Flowchart of the furnace-balancing procedure [57].

Meanwhile, to ensure the reliability of the SIS system, independent detection components, execution components, logic calculators, alarm and communication equipment should be installed, and each component should have a self-diagnosis function [97]. Furthermore, in the monitoring of key parameters such as the stator temperature of the compressor main motor, the pressure inside the furnace, steam pressure, water carbon ratio, and medium temperature, in order to prevent instrument failures or accuracy errors caused by long-term service from causing erroneous shutdowns, the dual three-channel redundant error tolerance system (DTRFS) architecture of SIS should be adopted [98, 99].

Fig. 10 presents the reliability block diagram of the DTRFS architecture. Only when the monitoring parameters of two or more instruments are judged to exceed the standard at the same time can the interlocking device be triggered, and the controller of the SIS system also adopts redundant configuration, reaching the SIL3 standard, to

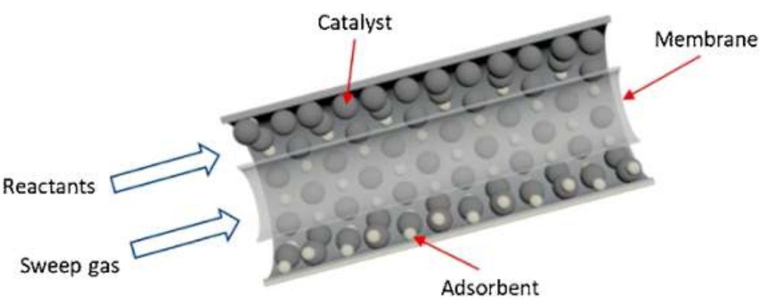

Figure 8. Scheme of MRR for hydrogen production from natural gas [94].

21969744, 0, Downloaded from https://onlinelibrary.wiley.com/doi/10.1002/cben.202300049 by China University Of Mining, Wiley Online Library on [31/01/2024]. See the Terms and Conditions (https://onlinelibrary.wiley.com/terms-and-conditions) on Wiley Online Library for rules of use; OA articles are governed by the applicable Creative Commons License

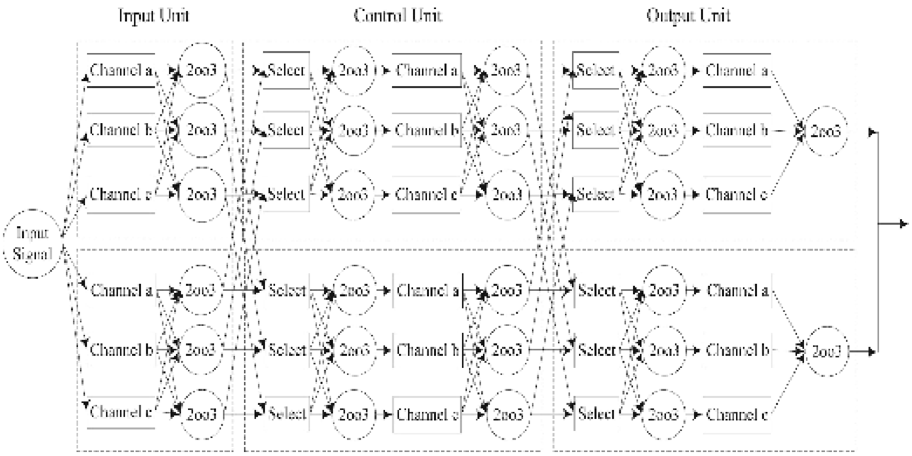

Figure 10. Reliability block diagram of the DTRFS architecture [99].

ensure the safe, efficient, and stable operation of the hydrogen production device for a long period of time [100].

The failure rate p of the non-redundant system is assumed to be 0.05 (i.e., reliability $R = 0.95$). Then according to Eq. (3), the reliability of the triple redundant system is $R = 0.999875$ and $p = 0.000125$, which is more than 99 % reduction in the failure rate.

$$R = 1 - \prod_{i=1}^{n} p_i \qquad (3)$$

The shutdown process of hydrogen production plants is also a complex system engineering. Improper operation can easily cause catalyst carbon deposition or poisoning, and can also lead to device damage or decreased service life, and even lead to serious safety and environmental accidents [101]. Tab. 6 shows the standardized shutdown steps of the NG hydrogen production system.

Summarizing the experience of device shutdown, it is necessary to focus on the protection of catalysts, hydrogen production conversion furnaces, furnace tubes, steam generators, and other equipment. For reforming furnaces and tubes, in order to reduce damage caused by thermal stress, the cooling rate must be strictly controlled (≤ 30 °C/h) during shutdown [102]. In order to maintain a uniform temperature field in the furnace during the process of shutting down the converter burner, the ceasefire sequence should be reasonably arranged according to the distribution of fire nozzles. At the same time, furnace pressure fluctuations should be controlled, as severe pressure fluctuations may cause catalyst breakage, which can lead to an increase in resistance and uneven temperature in the conversion tube after production recovery, producing bright spots or red tubes in the conversion tube. For steam generators, it is necessary to maintain a high liquid level in the steam drum during shutdown to prevent dry burning.

6.2 Fire and Explosion

6.2.1 Causes of an Accident

Fire and explosion are the most destructive types of accidents facing SMR processes. Hydrogen gas in hydrogen production equipment and pipelines can leak through small pores, and even penetrate from materials [103]. Hydrogen leakage generates escalation vectors (e.g., jet fires, steam cloud explosions), further causing damage to other equipment and endangering personnel safety.

Fig. 11 shows a flow chart from hydrogen leakage to occurrence of accidents. During the literature research process, it was found that the current behavior of hydrogen leakage, calculation of explosion overpressure, and determination of safety distance were mostly obtained through simulation software [104–108]. So far, the partial evolution mechanism of accidents is still unclear, such as the kinetic mechanism of high-pressure hydrogen leakage reaction and the synergistic damage effect of hydrogen and other components on materials, so further model optimization and on-site experiments are necessary [109].

6.2.2 Preventive Measures

To prevent such accidents from occurring, the key is to avoid hydrogen and oxygen mixing reaching the explosion limit, while also avoiding ignition sources [110]. So hydrogen leakage

Table 6. Shutdown steps of NG hydrogen production system.

Order	Operation content
1	Reduce temperature and load and cut off the preconversion reactor.
2	Interlock and shut down the boiler, cut off the feeding and hydrogen distribution, and isolate and relieve the pressure of the fuel gas system.
3	Stop supplying steam and water to the conversion system.
4	Pressure relief and nitrogen replacement of the conversion system.
5	Pressure relief and nitrogen replacement of the desulfurization system.
6	High-pressure steam drum steam production control, stop the machine and pump, and stop the PSA unit.

21969744, 0, Downloaded from https://onlinelibrary.wiley.com/doi/10.1002/cben.202300049 by China University Of Mining, Wiley Online Library on [31/01/2024]. See the Terms and Conditions (https://onlinelibrary.wiley.com/terms-and-conditions) on Wiley Online Library for rules of use; OA articles are governed by the applicable Creative Commons License

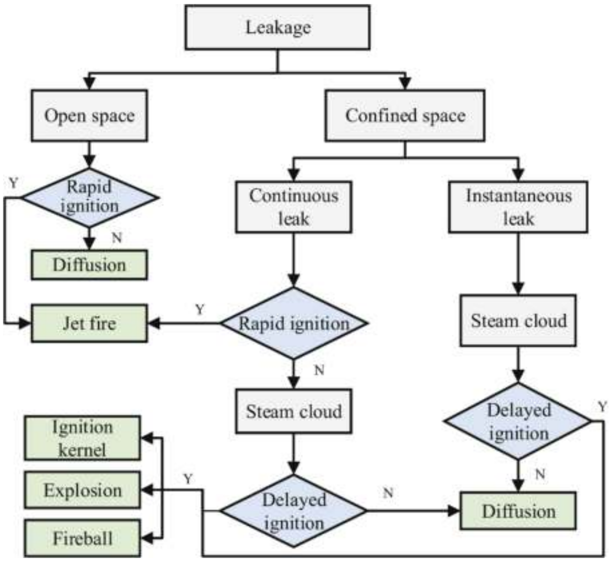

Figure 11. Flow chart of accidents due to hydrogen leakage [28].

should be detected and located in a timely manner. Sun et al. [111] demonstrated a fast response visual colorimetric hydrogen detector based on Pd/MoO_3 nanocomposites for hydrogen leakage monitoring. At 25 °C, when the H_2 concentration exceeds 1 %, these nanocomposites can exhibit a perceptible color change within 10 s. It can be used as an external surface coating for hydrogen production, storage equipment, and pipelines to quickly locate the leakage point after hydrogen leakage occurs. Moreover, installing hydrogen detectors and hydrogen flame detectors around the devices and equipping patrol personnel with portable combustible gas detectors, are basic monitoring and accident prevention measures. Oxygen content analyzers in the PSA unit and hydrogen storage container should be installed to achieve real-time monitoring of oxygen content and the health status of the devices. The detection data should be transmitted to the SIS system for real-time monitoring. Automatic sound and light alarms signal when abnormal situations occur.

Potential ignition sources within the factory area must be strictly controlled. For example, explosion-proof lamps should be selected, and the lamp should be installed in a lower position and away from gas release sources. Static electricity and lightning protection grounding devices should be installed in the hydrogen storage tank area [112]. During on-site operations, personnel should wear antistatic clothing, gloves, hats, and shoes to avoid generating static sparks. The environmental humidity should be appropriately adjusted. The power line adopts flame-retardant cables for transmission to prevent fire from spreading along the circuit, and is laid underground or overhead through steel pipes.

It should also be noted that before filling the device with hydrogen a leak detection should be conducted and the device should be thoroughly purged with N_2. The hydrogen-containing system needs to maintain a positive pressure state at all times. Ventilation devices for confined space should be provided where hydrogen may accumulate after leakage [113]. Hydrogen transmission pipelines and equipment should be connected using threaded joints, and the threaded joint should be filled with polytetrafluoroethylene that is resistant to hydrogen corrosion and high temperature.

6.2.3 Emergency Measures

In addition to the requirements for production standards, detailed emergency response equipment and plans should also be prepared. In order to prevent backfire during hydrogen release, the vent pipe of hydrogen storage vessels shall be equipped with a flame arrester or nitrogen purging device. In order to prevent rust friction sparks, the short vent pipe behind the flame arrester should be made of stainless steel. The vent pipe should be provided with safety measures against rain and snow intrusion and debris blockage. The hydrogen storage container should be supplied with bursting discs and safety valves, and the surrounding walls and vent ports should be set [114].

To timely extinguish initial and local fires, firstly, wheeled or portable dry powder fire extinguishers and carbon dioxide fire extinguishers should be equipped at key locations according to the layout of production equipment. Secondly, semi fixed fire extinguishing steam joints should be installed around the platforms of vertical equipment, multilayer framework platforms, and equipment with operating temperatures exceeding the spontaneous ignition point of reactants as needed. Thirdly, fire hose reels should be installed at key locations such as the hot oil pump, combustion furnace, and the lower part of the pipe bridge.

Diversified hydrogen explosion-proof technologies for different stages and scenarios are also being continuously explored in depth. Shang et al. [115] independently developed a set of hydrogen explosion suppression equipment and verified its performance. After receiving the flame sensor signal, the suppressant (perfluorohexanone-modified dry water) was sprayed into the explosion area to prevent further expansion of the hydrogen flame. Flames with a hydrogen equivalence ratio less than 0.5 were successfully suppressed. Long et al. [116] found that foam copper porous material has a quenching effect on H_2/CH_4 premixed explosions in barrier tubes, and the larger the porosity, the better the decompression and quenching effects.

Gao et al. [117] studied the influence of the morphology and location of obstacles around hydrogen storage tanks on hydrogen diffusion, and evaluated the protective effect of obstacles on workers and other equipments. Wu et al. [118] stated that the overall bending of hydrogen jet flames is the prerequisite for extinguishment. Wang et al. [119] found through experiments that adding N_2 and CO_2 to the H_2-LPG-air mixture can reduce the maximum explosion pressure and maximum pressure rise rate of the mixture, while also delaying the arrival of the explosion peak. The addition of CO_2 has a greater impact on the variation of the explosion pressure curve, as depicted in Fig. 12, which has a better effect on inhibiting explosions than N_2. These developments in explosion-proof technology add the final safety barrier to the hydrogen infrastructure. However, most of them are still in the stage of model validation and experimentation, lacking the evaluation of feasibility and effectiveness in specific scenarios.

21969744, 0, Downloaded from https://onlinelibrary.wiley.com/doi/10.1002/cben.202300049 by China University Of Mining, Wiley Online Library on [31/01/2024]. See the Terms and Conditions (https://onlinelibrary.wiley.com/terms-and-conditions) on Wiley Online Library for rules of use; OA articles are governed by the applicable Creative Commons License

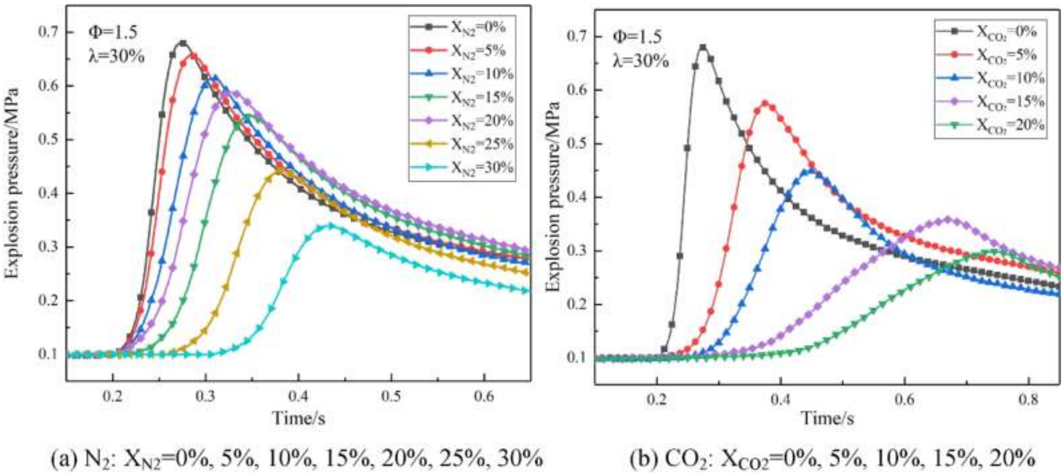

Figure 12. Explosion pressure curves of H_2-LPG-air mixtures under different inert gas proportions. (a) N_2; (b) CO_2 [119].

7 Discussion

Based on a comprehensive multi-criteria decision-making (MCDM) evaluation framework of efficiency, safety and infrastructure, the SMR process was assessed as the most desirable technology for hydrogen production [120]. Despite the relative maturity of the technology, improvements and enhancements from a safety perspective are still necessary. SMR is susceptible to fires and explosions, and the high temperatures and pressures of the operating conditions require more robust materials, better process control, and better emergency preparedness to minimize risk.

The material selection of the reaction vessel must give full consideration to the reaction conditions and the physical and chemical properties of the reaction medium. We provide an overview of the material selection requirements for critical reaction vessels and vulnerable parts, with a special emphasis on the importance of catalysts for safeguarding process. Proper material selection maintains process continuity and avoids unnecessary downtime losses and hazards caused by accidental release of reaction media. The decrease in the mechanical energy coefficient of reforming tubes and tanks is accompanied by an increase in the probability of damage and explosion [121]. It is noted that some material performance requirements apply equally to other hydrogen production programs and hydrogen energy infrastructure.

The safety optimization of process consists of two aspects: the mitigation of uncertainty and the reduction of potential accident energy. Improvement of the burner placement and feed distribution scheme in the reforming furnace to achieve proper temperature distribution can reduce the uncertainty caused by uneven heating. The optimization of predictive control algorithms for PSA can help reduce the uncertainty induced by various process disturbances. The structural modification of the burner reduces the uncertainty arising from insufficient supply of desorbed gas when the unit is started and stopped. The in-situ hydrogen separation function available in the MRR can continuously shift the thermodynamic equilibrium of SMR reaction towards the product direction [122]. Thus, this process intensification requires lower heat consumption than traditional reactors to achieve the same hydrogen yield target. In addition to reducing energy consumption costs, it also provides safer and milder reaction conditions, i.e., lower temperature and pressure.

Simulation results from mathematical models have confirmed the economic and technical advantages (e.g., optimal gas-catalyst contact, heat management, reduced bed-to-membrane mass transfer limitations) of the MRR scheme [123]. In summary, the operating conditions of the MRR reduce the potential accident energy. Nevertheless, more pilot experimental data are needed to confirm the stability, reliability, and longevity of MRR under normal operating conditions.

A reliable SIS maintains processes that deviate from normal operating conditions in a safe manner. Redundant component configurations compensate for reliability degradation caused by degraded components that are not detected in time [124]. Redundant monitor deployment can also reduce the probability of automated decisions issuing incorrect instructions. With regard to emergency process termination, we also emphasize the correct sequence of operations and key points of protection for the device.

Fires and explosions are the most destructive accident scenarios facing hydrogen production processes. There are complex interactions and uncertainties between fires and explosions caused by hydrogen leaks [125]. Once the safety barrier has failed, thermal radiation, overpressure, or blast fragments can rapidly expand the accident further from the initial unit to the surrounding area.

We systematically survey traditional and latest technologies for leak monitoring, ignition source management, and explosion protection. Further development of explosion protection technology depends on the exploration of the mechanisms of hydrogen accident evolution and leakage dynamics. The effectiveness of their selection and combined application for controlling risk also requires further experimental and modeling evaluation.

21969744, 0, Downloaded from https://onlinelibrary.wiley.com/doi/10.1002/cben.202300049 by China University Of Mining, Wiley Online Library on [31/01/2024]. See the Terms and Conditions (https://onlinelibrary.wiley.com/terms-and-conditions) on Wiley Online Library for rules of use; OA articles are governed by the applicable Creative Commons License

8 Outlook

The high complexity and increasing interdependence of hydrogen production facilities make them increasingly susceptible to the domino effect. The relevant accident cases exhibit the characteristics of low frequency and high consequences. The operation of SMR facilities requires high levels of safety and reliability. This cannot be separated from the demand for efficient and effective process safety and risk management technologies, which will greatly reduce the probability and consequences of potential accidents.

The SMR system can improve safety and reliability by:

(1) Conducting in-depth research on the damage propagation and failure mechanisms of equipment and materials in hydrogen environments.

(2) Improving quantitative evaluation methods for hydrogen damage, and accelerating the development of new materials with high reliability and long-term hydrogen corrosion resistance.

(3) Implementing more medium- and large-scale hydrogen infrastructure (e.g., production line, transmission pipeline, storage tank) accident experiments to enrich the relevant databases in order to validate and optimize existing accident and risk assessment models.

(4) Developing commercially available Pd-based membranes and MRR to replace existing reforming furnace for hydrogen production at lower temperatures and pressures.

9 Conclusion

Natural gas steam reforming for hydrogen production has the advantages of low comprehensive energy consumption, high hydrogen production efficiency, and low cost under existing technological conditions. In the process of developing a low-carbon economy, this technology can achieve a smooth transition between fossil energy and renewable energy systems. After long-term production practice in chemical enterprises, a series of measures have been taken to improve and innovate the inherent safety and long-term operation of NG reforming hydrogen production technology, resulting in a significant improvement in the overall safety level of the technology.

However, the current safety and emergency support technology system still faces enormous challenges, and it is necessary to carry out research and development from the technology level. Specific research demands are as follows:

(1) The SIS system is prone to delays and false alarms due to the lack of a sufficient number of samples of anomalous operating conditions, as well as data "noisy" interferences caused by fluctuations in the reactants quality and deficiencies in the monitors performance. Optimization of judgment algorithms and redundant configuration of components can be attempted to enhance the reliability of the SIS system.

(2) There are few effective technologies available to prevent spontaneous combustion after leakage of high-pressure hydrogen, and more research should be conducted on this topic, such as developing safe and rapid release technologies that use CO_2 to suppress premixed gas flames.

(3) At present, research on catalysts for hydrogen production from NG is not sufficient. By introducing active metals or adjusting the physicochemical properties of carriers, it is expected to further improve the efficiency and safety of hydrogen production processes.

(4) CFD simulations can be used to improve the burner placement and feed distribution scheme, so that proper temperature distribution inside the reforming furnace can be achieved and premature catalyst and reforming tubes failure can be avoided.

Conflicts of Interest

The authors declare no conflict of interest.

Lele Feng received his B.S. and Ph.D. degrees from the Tsinghua University in 2015 and 2020, respectively. He is now working at the China University of Mining and Technology (CUMT) and is mainly engaged in the research of low-carbon utilization of solid fuels and in-situ gasification of coal for hydrogen production.

Acknowledgment

The support provided by the National Natural Science Foundation of China (Grant No. 52106189) and by the Shuangchuang Doctor Project of Jiangsu Province (202131196) is highly appreciated. This research was also financially supported by funding from the Key Laboratory of Hubei Province for Coal Conversion and New Carbon Materials (Wuhan University of Science and Technology), Grant No. WKDM202302.

Abbreviations

ATR	autothermal reforming
BET	Brunauer-Emmett-Teller
BN	Bayesian network
BWM	best-worst method
CCU	carbon capture and utilization
DBN	dynamic Bayesian network
DNT	D number theory
ESD	emergency shutdown device
ETA	event tree analysis
FSEM	fire synergistic effect model
FST	fuzzy set theory
HAZOP	hazard and operability
MPC	model predictive control

© 2024 Wiley-VCH GmbH

21969744, 0, Downloaded from https://onlinelibrary.wiley.com/doi/10.1002/cben.202300049 by China University Of Mining, Wiley Online Library on [31/01/2024]. See the Terms and Conditions (https://onlinelibrary.wiley.com/terms-and-conditions) on Wiley Online Library for rules of use; OA articles are governed by the applicable Creative Commons License

MRR membrane-integrated reformer reactor
NG natural gas
OTWT outer tube wall temperature
POX partial oxidation
PRA preliminary risk analysis
PSA pressure swing adsorption
SIS safety instrumented system
SMR steam methane reforming

References

[1] S. A. Hussain, F. Razi, K. Hewage, R. Sadiq, The perspective of energy poverty and 1st energy crisis of green transition, *Energy* **2023**, *275*, 127487. DOI: https://doi.org/10.1016/j.energy.2023.127487

[2] A. Zerboni, T. Rossi, R. Bengalli, T. Catelani, C. Rizzi, M. Priola, S. Casadei, P. Mantecca, Diesel exhaust particulate emissions and in vitro toxicity from Euro 3 and Euro 6 vehicles, *Environ. Pollut.* **2022**, *297*, 118767. DOI: https://doi.org/10.1016/j.envpol.2021.118767

[3] M. D. G. Rivas, J. Gonzalo, Trends in distributional characteristics: Existence of global warming, *J. Econometrics* **2020**, *214 (1)*, 153–174. DOI: https://doi.org/10.1016/j.jeconom.2019.05.009

[4] Q. I. Roode-Gutzmer, D. Kaiser, M. Bertau, Renewable methanol synthesis, *ChemBioEng Rev.* **2019**, *6 (6)*, 209–236. DOI: https://doi.org/10.1002/cben.201900012

[5] M. Amin, H. H. Shah, A. G. Fareed, W. U. Khan, E. Chung, A. Zia, Z. U. R. Farooqi, C. Lee, Hydrogen production through renewable and non-renewable energy processes and their impact on climate change, *Int. J. Hydrogen Energy* **2022**, *47 (77)*, 33112–33134. DOI: https://doi.org/10.1016/j.ijhydene.2022.07.172

[6] J. Choi, D. G. Choi, S. Y. Park, Analysis of effects of the hydrogen supply chain on the Korean energy system, *Int. J. Hydrogen Energy* **2022**, *47 (52)*, 21908–21922. DOI: https://doi.org/10.1016/j.ijhydene.2022.05.033

[7] Q. Hassan, A. Z. Sameen, H. M. Salman, M. Jaszczur, M. Al-Hitmi, M. Alghoul, Energy futures and green hydrogen production, Is Saudi Arabia trend?, *Results Eng.* **2023**, *18*, 101165. DOI: https://doi.org/10.1016/j.rineng.2023.101165

[8] X.-Y. Pan, G. Yuan, X.-H. Wu, P.-J. Xie, The effects of government subsidies on the economic profits of hydrogen energy enterprises – An analysis based on A-share listed enterprises in China, *Renewable Energy* **2023**, *211*, 445–451. DOI: https://doi.org/10.1016/j.renene.2023.04.093

[9] P.-K. Liu, X. Han, Comparative analysis on similarities and differences of hydrogen energy development in the World's top 4 largest economies: A novel framework, *Int. J. Hydrogen Energy* **2022**, *47 (16)*, 9485–9503. DOI: https://doi.org/10.1016/j.ijhydene.2022.01.038

[10] D. Khatiwada, R. A. Vasudevan, B. H. Santos, Decarbonization of natural gas systems in the EU –costs, barriers, and constraints of hydrogen production with a case study in Portugal, *Renewable Sustainable Energy Rev.* **2022**, *168*, 112775. DOI: https://doi.org/10.1016/j.rser.2022.112775

[11] A. Ozawa, T. Tsani, Y. Kudoh, Japan's pathways to achieve carbon neutrality by 2050 – Scenario analysis using an energy modeling methodology, *Renewable Sustainable Energy Rev.* **2022**, *169*, 112943. DOI: https://doi.org/10.1016/j.rser.2022.112943

[12] A. Midilli, H. Kucuk, M. E. Topal, U. Akbulut, I. Dincer, A comprehensive review on hydrogen production from coal gasification: Challenges and opportunities, *Int. J. Hydrogen Energy* **2021**, *46 (50)*, 25385–25412. DOI: https://doi.org/10.1016/j.ijhydene.2021.05.088

[13] M. Younas, S. Shafique, A. Hafeez, F. Javed, F. Rehman, An overview of hydrogen production: current status, potential, and challenges, *Fuel* **2022**, *316*, 123317. DOI: https://doi.org/10.1016/j.fuel.2022.123317

[14] J. D. Holladay, J. Hu, D. L. King, Y. Wang, An overview of hydrogen production technologies, *Catal. Today* **2009**, *139 (4)*, 244–260. DOI: https://doi.org/10.1016/j.cattod.2008.08.039

[15] X.-X. Xu, Q. Zhou, D.-H. Yu, The future of hydrogen energy: Bio-hydrogen production technology, *Int. J. Hydrogen Energy* **2022**, *47 (79)*, 33677–33698. DOI: https://doi.org/10.1016/j.ijhydene.2022.07.261

[16] S. A. Ikonnikova, B. R. Scanlon, S. A. Berdysheva, A global energy system perspective on hydrogen Trade: A framework for the market color and the size analysis, *Appl. Energy* **2023**, *330*, 120267. DOI: https://doi.org/10.1016/j.apenergy.2022.120267

[17] K.-Y. Dong, R.-J. Sun, J. Wu, G. Hochman, The growth and development of natural gas supply chains: The case of China and the US, *Energy Policy* **2018**, *123*, 64–71. DOI: https://doi.org/10.1016/j.enpol.2018.08.034

[18] A.-L. Jia, G. Cheng, W.-Y. Chen, Y.-L. Li, Forecast of natural gas supply and demand in China under the background of "Dual Carbon Targets", *Pet. Explor. Dev.* **2023**, *50 (2)*, 492–504. DOI: https://doi.org/10.1016/S1876-3804(23)60404-5

[19] S. Schneider, S. Bajohr, F. Graf, T. Kolb, State of the art of hydrogen production via pyrolysis of natural gas, *ChemBioEng Rev.* **2020**, *7 (5)*, 150–158. DOI: https://doi.org/10.1002/cben.202000014

[20] S.-J. Chen, Q.-H. Zhang, H. D. Nguyen, Y.-Z. Ren, Y.-M. Liu, W. Wang, W.-C. Gao, J.-W. Ren, K. Sagoe-Crentsil, W.-H. Duan, Direct 2D cement-nanoadditive deposition enabling carbon-neutral hydrogen from natural gas, *Nano Energy* **2022**, *99*, 107415. DOI: https://doi.org/10.1016/j.nanoen.2022.107415

[21] E. Heo, J. Kim, S. Cho, Selecting hydrogen production methods using fuzzy analytic hierarchy process with opportunities, costs, and risks, *Int. J. Hydrogen Energy* **2012**, *37 (23)*, 17655–17662. DOI: https://doi.org/10.1016/j.ijhydene.2012.09.055

[22] E. Kawai, A. Ozawa, B. D. Leibowicz, Role of carbon capture and utilization (CCU) for decarbonization of industrial sector: A case study of Japan, *Appl. Energy* **2022**, *328*, 120183. DOI: https://doi.org/10.1016/j.apenergy.2022.120183

[23] S. M. Ali, I. I. I. Alkhatib, A. AlHajaj, L. F. Vega, How sustainable and profitable are large-scale hydrogen production plants from CH_4 and H_2S?, *J. Cleaner Prod.* **2023**, *428*, 139475. DOI: https://doi.org/10.1016/j.jclepro.2023.139475

[24] N. Ade, A. Alsuhaibani, M. M. El-Halwagi, H. Goyette, B. Wilhite, Integrating safety and economics in designing a

21969744, 0, Downloaded from https://onlinelibrary.wiley.com/doi/10.1002/cben.202300049 by China University Of Mining, Wiley Online Library on [31/01/2024]. See the Terms and Conditions (https://onlinelibrary.wiley.com/terms-and-conditions) on Wiley Online Library for rules of use; OA articles are governed by the applicable Creative Commons License

steam methane reforming process, *Int. J. Hydrogen Energy* **2022**, *47 (9)*, 6404–6414. DOI: https://doi.org/10.1016/j.ijhydene.2021.11.240
[25] C.-H. Song, H.-P. Jiang, W. Gao, High temperature generated by sliding metal friction and its effectiveness as an ignition source for hydrogen, *J. Loss Prev. Process Ind.* **2022**, *79*, 104833. DOI: https://doi.org/10.1016/j.jlp.2022.104833
[26] L.-Q. Wang, H.-H. Ma, Z.-W. Shen, J. Pan, A comparative study of the explosion behaviors of H_2 and C_2H_4 with air, N_2O and O_2, *Fire Saf. J.* **2021**, *119*, 103260. DOI: https://doi.org/10.1016/j.firesaf.2020.103260
[27] W.-G. Cao, Z.-H. Zhou, W.-J. Li, Y.-M. Zhao, Z.-X. Yang, Y. Zhang, S.-M. Ouyang, C.-M. Shu, Y.-X. Tan, Under-expansion jet flame propagation characteristics of premixed H_2/air in explosion venting, *Int. J. Hydrogen Energy* **2021**, *46 (78)*, 38913–38922. DOI: https://doi.org/10.1016/j.ijhydene.2021.09.109
[28] F.-Y. Yang, T.-Z. Wang, X.-T. Deng, J. Dang, Z.-Y. Huang, S. Hu, Y.-Y. Li, M.-G. Ouyang, Review on hydrogen safety issues: Incident statistics, hydrogen diffusion, and detonation process, *Int. J. Hydrogen Energy* **2021**, *46 (61)*, 31467–31488. DOI: https://doi.org/10.1016/j.ijhydene.2021.07.005
[29] N. Norazahar, T. M. Ambikabathy, R. M. Kasmani, A. Ahmad, A. A. Jalil, T. A. T. Abdullah, M. F. A. Kamaroddin, Hydrogen application and its safety: An overview of public perceptions and acceptance in Malaysia, *Process Saf. Environ. Prot.* **2023**, *180*, 686–698. DOI: https://doi.org/10.1016/j.psep.2023.10.019
[30] Q. Tong, T. Gernay, Resilience assessment of process industry facilities using dynamic Bayesian networks, *Process Saf. Environ. Prot.* **2023**, *169*, 547–563. DOI: https://doi.org/10.1016/j.psep.2022.11.048
[31] V. Cozzani, G. Gubinelli, E. Salzano, Escalation thresholds in the assessment of domino accidental events, *J. Hazard. Mater.* **2006**, *129 (1–3)*, 1–21. DOI: https://doi.org/10.1016/j.jhazmat.2005.08.012
[32] O. A. Rosyid, D. Jablonski, U. Hauptmanns, Risk analysis for the infrastructure of a hydrogen economy, *Int. J. Hydrogen Energy* **2007**, *32 (15)*, 3194–3200. DOI: https://doi.org/10.1016/j.ijhydene.2007.02.012
[33] M. Moonis, A. J. Wilday, M. J. Wardman, Semi-quantitative risk assessment of commercial scale supply chain of hydrogen fuel and implications for industry and society, *Process Saf. Environ. Prot.* **2010**, *88 (2)*, 97–108. DOI: https://doi.org/10.1016/j.psep.2009.11.006
[34] I. Mohammadfam, E. Zarei, Safety risk modeling and major accidents analysis of hydrogen and natural gas releases: A comprehensive risk analysis framework, *Int. J. Hydrogen Energy* **2015**, *40 (39)*, 13653–13663. DOI: https://doi.org/10.1016/j.ijhydene.2015.07.117
[35] *Bayesian Networks and Decision Graphs* (Eds: F. V. Jensen, T. D. Nielsen), Vol. 2, Springer, New York **2007**. DOI: https://doi.org/10.1007/978-0-387-68282-2
[36] D. Marquez, M. Neil, N. Fenton, Improved reliability modeling using Bayesian networks and dynamic discretization, *Reliab. Eng. Syst. Saf.* **2010**, *95 (4)*, 412–425. DOI: https://doi.org/10.1016/j.ress.2009.11.012
[37] N. Khakzad, Application of dynamic Bayesian network to risk analysis of domino effects in chemical infrastructures, *Reliab. Eng. Syst. Saf.* **2015**, *138*, 263–272. DOI: https://doi.org/10.1016/j.ress.2015.02.007
[38] S. A. Adedigba, F. Khan, M. Yang, An integrated approach for dynamic economic risk assessment of process systems, *Reliab. Eng. Syst. Saf.* **2018**, *116*, 312–323. DOI: https://doi.org/10.1016/j.psep.2018.01.013
[39] X.-X. Guo, J. Ji, F. Khan, L. Ding, Q. Tong, A novel fuzzy dynamic Bayesian network for dynamic risk assessment and uncertainty propagation quantification in uncertainty environment, *Saf. Sci.* **2021**, *141*, 105285. DOI: https://doi.org/10.1016/j.ssci.2021.105285
[40] E. Zarei, F. Khan, M. Yazdi, A dynamic risk model to analyze hydrogen infrastructure, *Int. J. Hydrogen Energy* **2021**, *46 (5)*, 4626–4643. DOI: https://doi.org/10.1016/j.ijhydene.2020.10.191
[41] M. T. Amin, F. Khan, S. Z. Halim, S. Pistikopoulos, A holistic framework for process safety and security analysis, *Comput. Chem. Eng.* **2022**, *165*, 107963. DOI: https://doi.org/10.1016/j.compchemeng.2022.107963
[42] K.-X. Huang, G.-H. Chen, F. Khan, Vulnerability assessment method for domino effects analysis in chemical clusters, *Process Saf. Environ. Prot.* **2022**, *164*, 539–554. DOI: https://doi.org/10.1016/j.psep.2022.06.021
[43] L. Ding, F. Khan, J. Ji, A novel approach for domino effects modeling and risk analysis based on synergistic effect and accident evidence, *Reliab. Eng. Syst. Saf.* **2020**, *203*, 107109. DOI: https://doi.org/10.1016/j.ress.2020.107109
[44] X. Peng, Q.-B. Jin, Molecular simulation of methane steam reforming reaction for hydrogen production, *Int. J. Hydrogen Energy* **2022**, *47 (12)*, 7569–7585. DOI: https://doi.org/10.1016/j.ijhydene.2021.12.105
[45] A. M. Starik, P. S. Kuleshov, B. I. Loukhovitski, N. S. Titova, Theoretical study of partial oxidation of methane by non-equilibrium oxygen plasma to produce hydrogen rich syngas, *Int. J. Hydrogen Energy* **2015**, *40 (32)*, 9872–9884. DOI: https://doi.org/10.1016/j.ijhydene.2015.06.066
[46] P. M. Araújo, K. M. D. Costa, F. B. Passos, Hydrogen production from methane autothermal reforming over $CaTiO_3$, $BaTiO_3$ and $SrTiO_3$ supported nickel catalysts, *Int. J. Hydrogen Energy* **2021**, *46 (47)*, 24107–24116. DOI: https://doi.org/10.1016/j.ijhydene.2021.04.202
[47] A. Boyano, T. Morosuk, A. M. Blanco-Marigorta, G. Tsatsaronis, Conventional and advanced exergoenvironmental analysis of a steam methane reforming reactor for hydrogen production, *J. Cleaner Prod.* **2012**, *20 (1)*, 152–160. DOI: https://doi.org/10.1016/j.jclepro.2011.07.027
[48] K.-W. Li, B. Yu, T. Zhang, Economic analysis of hydrogen production from steam reforming process: A literature review, *Energy Sources, Part B* **2018**, *13 (2)*, 109–115. DOI: https://doi.org/10.1080/15567249.2017.1387619
[49] A. Amini, A. A. H. Bagheri, M. H. Sedaghat, M. R. Rahimpour, CFD simulation of an industrial steam methane reformer: Effect of burner fuel distribution on hydrogen production, *Fuel* **2023**, *352*, 129008. DOI: https://doi.org/10.1016/j.fuel.2023.129008
[50] B. O. A. Sasi, A. Demirbas, Removal of sulfur from sulfur-bearing natural gas to produce clean jet fuel, *Pet. Sci. Technol.* **2016**, *34 (17–18)*, 1550–1555. DOI: https://doi.org/10.1080/10916466.2016.1214598

21969744, 0, Downloaded from https://onlinelibrary.wiley.com/doi/10.1002/cben.202300049 by China University Of Mining, Wiley Online Library on [31/01/2024]. See the Terms and Conditions (https://onlinelibrary.wiley.com/terms-and-conditions) on Wiley Online Library for rules of use; OA articles are governed by the applicable Creative Commons License

[51] J. G. Seo, M. H. Youn, J. C. Jung, K. M. Cho, S. Park, I. K. Song, Preparation of Ni/Al_2O_3-ZrO_2 catalysts and their application to hydrogen production by steam reforming of LNG: Effect of ZrO_2 content grafted on Al_2O_3, *Catal. Today* **2008**, *138 (3–4)*, 130–134. DOI: https://doi.org/10.1016/j.cattod.2008.05.006

[52] A. Amini, M. H. Sedaghat, S. Jamshidi, A. Shariati, M. R. Rahimpour, A comprehensive CFD simulation of an industrial-scale side-fired steam methane reformer to enhance hydrogen production, *Chem. Eng. Process.* **2023**, *184*, 109269. DOI: https://doi.org/10.1016/j.cep.2023.109269

[53] X.-Y. Wang, C.-S. Zhang, W. Gao, Risk assessment of hydrogen leakage in diesel hydrogenation process, *Int. J. Hydrogen Energy* **2022**, *47 (10)*, 6955–6964. DOI: https://doi.org/10.1016/j.ijhydene.2021.12.027

[54] Y. Matsumura, T. Nakamori, Steam reforming of methane over nickel catalysts at low reaction temperature, *Appl. Catal., A* **2004**, *258 (1)*, 107–114. DOI: https://doi.org/10.1016/j.apcata.2003.08.009

[55] P. Chen, W. Du, M.-H. Zhang, F.-Y. Duan, L.-F. Zhang, Numerical studies on heat coupling and configuration optimization in an industrial hydrogen production reformer, *Int. J. Hydrogen Energy* **2019**, *44 (30)*, 15704–15720. DOI: https://doi.org/10.1016/j.ijhydene.2018.10.238

[56] J. Yun, Y. Kim, S. Yu, Interactive heat transfer characteristics of 5 kW class shell-and-tube methane steam reformer with intermediate temperature heat source, *Int. J. Hydrogen Energy* **2020**, *45 (41)*, 21767–21778. DOI: https://doi.org/10.1016/j.ijhydene.2020.05.152

[57] A. Tran, M. Pont, M. Crose, P. D. Christofides, Real-time furnace balancing of steam methane reforming furnaces, *Chem. Eng. Res. Des.* **2018**, *134*, 238–256. DOI: https://doi.org/10.1016/j.cherd.2018.03.032

[58] M. L. C. Nascimento, F. D. C. Gallo, F. D. S. Queiroz, M. C. Mendes, C. B. Eckstein, L. Nogueira Jr., I. L. May, G. R. Pereira, L. H. D. Almeida, Effect of short-time overheating in the morphology of primary carbides network in Nb and NbTi-modified HP stainless steels steam reforming tubes, *J. Mater. Res. Technol.* **2023**, *22*, 382–392. DOI: https://doi.org/10.1016/j.jmrt.2022.11.130

[59] M.-S. Wang, D. Flahaut, Z. Zhang, I. P. Jones, Y. L. Chiu, Primary carbide transformation in a high performance micro-alloy at 1000 °C, *J. Alloys Compd.* **2019**, *781*, 751–760. DOI: https://doi.org/10.1016/j.jallcom.2018.12.095

[60] J. Yun, S. Yu, Transient behavior of 5 kW class shell-and-tube methane steam reformer with intermediate temperature heat source, *Int. J. Heat Mass Transfer* **2019**, *134*, 600–609. DOI: https://doi.org/10.1016/j.ijheatmasstransfer.2019.01.078

[61] B. Ensor, The effect of varying nickel concentration on the hydrogen pickup fraction and corrosion resistance in Zircaloy-4, *J. Nucl. Mater.* **2023**, *574*, 154149. DOI: https://doi.org/10.1016/j.jnucmat.2022.154149

[62] H. Ebrahimi, A. Zamaniyan, R. Hosseini, K. Forsat, Analysis of reformer furnace tubes for hydrogen production using radiative zonal model, *Int. J. Hydrogen Energy* **2014**, *39 (25)*, 13164–13173. DOI: https://doi.org/10.1016/j.ijhydene.2014.06.131

[63] W. G. Bareiro, F. D. A. Silva, E. D. Sotelino, Thermo-mechanical behavior of stainless steel fiber reinforced refractory concrete: Experimental and numerical analysis, *Constr. Build. Mater.* **2020**, *240*, 117881. DOI: https://doi.org/10.1016/j.conbuildmat.2019.117881

[64] C.-H. Xu, L. Wang, Z.-C. Yu, P.-H. Ge, T.-T. Li, X.-T. Yue, X.-Q. Wang, Characterization of flexible aluminosilicate bulk fibers and fibrous mats fabricated by facile electrospinning, *Ceram. Int.* **2023**, *49 (11)*, 17660–17667. DOI: https://doi.org/10.1016/j.ceramint.2023.02.132

[65] J. E. C. Lopez, M. P. Arenas, C. J. Pacheco, F. S. Queiroz, C. B. Eckstein, L. Nogueira, L. H. D. Almeida, J. M. A. Rebello, G. R. Pereira, Development of a magnetic sensor for detection of moderate carburization damages in heat-resistant HP-Nb tubes of steam reforming furnaces, *J. Mater. Res. Technol.* **2018**, *7 (3)*, 371–375. DOI: https://doi.org/10.1016/j.jmrt.2018.06.007

[66] M. Fabrik, A. Salama, H. Ibrahim, Modeling of catalyst poisoning during hydrogen production via methane steam and dry reforming, *Fuel* **2023**, *347*, 128429. DOI: https://doi.org/10.1016/j.fuel.2023.128429

[67] P. Forzatti, L. Lietti, Catalyst deactivation, *Catal. Today* **1999**, *52 (2–3)*, 165–181. DOI: https://doi.org/10.1016/S0920-5861(99)00074-7

[68] E. Meloni, M. Martino, V. Palma, A short review on Ni-based catalysts and related engineering issues for methane steam reforming, *Catalysts* **2020**, *10 (3)*, 352. DOI: https://doi.org/10.3390/catal10030352

[69] H. Khosravani, M. Meshksar, M. Koohi-Saadi, K. Taghadom, M. R. Rahimpour, Synthesis, characterization, and application of bio-templated Ni–Ce/Al_2O_3 catalyst for clean H_2 production in the steam reforming of methane process, *J. Energy Inst.* **2023**, *108*, 101203. DOI: https://doi.org/10.1016/j.joei.2023.101203

[70] S.-Q. Wang, S. A. Nabavi, P. T. Clough, A review on bipolymetallic catalysts for steam methane reforming, *Int. J. Hydrogen Energy* **2023**, *48 (42)*, 15879–15893. DOI: https://doi.org/10.1016/j.ijhydene.2023.01.034

[71] D. Batebi, R. Abedini, A. Mosayebi, Combined steam and CO_2 reforming of methane (CSCRM) over Ni–Pd/Al_2O_3 catalyst for syngas formation, *Int. J. Hydrogen Energy* **2020**, *45 (28)*, 14293–14310. DOI: https://doi.org/10.1016/j.ijhydene.2020.03.137

[72] M. H. S. Garai, M. R. Khosravi-Nikou, A. Shariati, Chemical looping steam methane reforming via Ni-ferrite supported on cerium and zirconium oxides, *Chem. Eng. Technol.* **2020**, *43 (9)*, 1813–1822. DOI: https://doi.org/10.1002/ceat.202000054

[73] M. V. Tsodikov, S. S. Kurdymov, G. I. Konstantinov, V. Y. Murzin, O. V. Bukhtenko, Y. V. Maksimov, Core-shell bifunctional catalyst for steam methane reforming resistant to H_2S: Activity and structure evolution, *Int. J. Hydrogen Energy* **2015**, *40 (7)*, 2963–2970. DOI: https://doi.org/10.1016/j.ijhydene.2015.01.016

[74] Y. Xu, T. Hirano, H. Kunieda, Y. Hara, Y. Miyata, Enhancing the methane steam reforming catalytic performance of Ni monolithic catalysts via Ni–Re surface alloying, *Catal. Sci. Technol.* **2020**, *10 (7)*, 2004–2019. DOI: https://doi.org/10.1039/C9CY02539A

 © 2024 Wiley-VCH GmbH

21969744, 0, Downloaded from https://onlinelibrary.wiley.com/doi/10.1002/cben.202300049 by China University Of Mining, Wiley Online Library on [31/01/2024]. See the Terms and Conditions (https://onlinelibrary.wiley.com/terms-and-conditions) on Wiley Online Library for rules of use; OA articles are governed by the applicable Creative Commons License

[75] A. H. Dam, H.-M. Wang, R. Dehghan-Niri, X.-F. Yu, J. C. Walmsley, A. Holmen, J. Yang, D. Chen, Methane activation on bimetallic catalysts: Properties and functions of surface Ni–Ag alloy, *ChemCatChem* **2019**, *11 (15)*, 3401–3412. DOI: https://doi.org/10.1002/cctc.201900679

[76] F. Morales-Cano, L. F. Lundegaard, R. R. Tiruvalam, H. Falsig, M. S. Skjøth-Rasmussen, Improving the sintering resistance of Ni/Al_2O_3 steam-reforming catalysts by promotion with noble metals, *Appl. Catal., A* **2015**, *498*, 117–125. DOI: https://doi.org/10.1016/j.apcata.2015.03.016

[77] A. M. Ribeiro, C. A. Grande, F. V. S. Lopes, J. M. Loureiro, A. E. Rodrigues, A parametric study of layered bed PSA for hydrogen purification, *Chem. Eng. Sci.* **2008**, *63 (21)*, 5258–5273. DOI: https://doi.org/10.1016/j.ces.2008.07.017

[78] S.-G. Jia, Q.-H. Tan, J.-Y. Ye, Z.-W. Zhu, Z.-G. Jiang, Experiments on dynamic mechanical properties of austenitic stainless steel S30408 and S31608, *J. Constr. Steel Res.* **2021**, *179*, 106556. DOI: https://doi.org/10.1016/j.jcsr.2021.106556

[79] M. Luberti, H. Ahn, Review of Polybed pressure swing adsorption for hydrogen purification, *Int. J. Hydrogen Energy* **2022**, *47 (20)*, 10911–10933. DOI: https://doi.org/10.1016/j.ijhydene.2022.01.147

[80] X.-Q. Zhu, X.-W. Wang, Experimental study of a rotary valve multi-bed rapid cycle pressure swing adsorption process based medical oxygen concentrator, *Adsorption* **2020**, *26 (8)*, 1267–1274. DOI: https://doi.org/10.1007/s10450-020-00240-5

[81] T. Tian, Y.-Y. Wang, B. Liu, Z.-Y. Ding, X.-X. Xu, M.-S. Shi, J. Ma, Y.-J. Zhang, D.-H. Zhang, Simulation and experiment of six-bed PSA process for air separation with rotating distribution valve, *Chin. J. Chem. Eng.* **2022**, *42*, 329–337. DOI: https://doi.org/10.1016/j.cjche.2021.03.027

[82] Y. Li, R. Liu, G. McRae, M. X. Yao, Corrosion performance of valve seat hardfacing materials in amine environment of boiler feed water service, *Prot. Met. Phys. Chem. Surf.* **2019**, *55 (2)*, 377–388. DOI: https://doi.org/10.1134/S2070205119020187

[83] B. Bai, R. Hu, C.-Y. Zhang, J. Xue, W. Yang, Effect of precipitates on hardening of 17-4PH martensitic stainless steel serviced at 300 °C in nuclear power plant, *Ann. Nucl. Energy* **2021**, *154*, 108123. DOI: https://doi.org/10.1016/j.anucene.2020.108123

[84] H.-Y. Si, L.-H. Cao, P. Li, D.-C. Chen, Vapor-liquid two-phase flow and thermodynamic loss of multi-stage high temperature and pressure reducing valve based on evaporation model, *Int. Commun. Heat Mass Transfer* **2023**, *147*, 106993. DOI: https://doi.org/10.1016/j.icheatmasstransfer.2023.106993

[85] M. A. F. Martins, A. E. Rodrigues, J. M. Loureiro, A. M. Ribeiro, I. B. R. Nogueira, Handling model uncertainty in control of a pressure swing adsorption unit for syngas purification: A multi-model zone control scheme-based robust model predictive control strategy, *Sep. Purif. Technol.* **2023**, *306*, 122668. DOI: https://doi.org/10.1016/j.seppur.2022.122668

[86] A. Caravella, G. Barbieri, E. Drioli, Theoretical study of H_2 permeation through supported Pd-based membranes, *Desalination* **2006**, *200 (1–3)*, 242–244. DOI: https://doi.org/10.1016/j.desal.2006.03.311

[87] S. M. Jokar, A. Farokhnia, M. Tavakolian, M. Pejman, P. Parvasi, J. Javanmardi, F. Zare, M. C. Gonçalves, A. Basile, The recent areas of applicability of palladium based membrane technologies for hydrogen production from methane and natural gas: A review, *Int. J. Hydrogen Energy* **2023**, *48 (16)*, 6451–6476. DOI: https://doi.org/10.1016/j.ijhydene.2022.05.296

[88] H. Li, H.-Y. Xu, W.-Z. Li, Study of n value and α/β palladium hydride phase transition within the ultra-thin palladium composite membrane, *J. Membr. Sci.* **2008**, *324 (1–2)*, 44–49. DOI: https://doi.org/10.1016/j.memsci.2008.06.053

[89] O. Iyoha, R. Enick, R. Killmeyer, B. Morreale, The influence of hydrogen sulfide-to-hydrogen partial pressure ratio on the sulfidization of Pd and 70 mol% Pd–Cu membranes, *J. Membr. Sci.* **2007**, *305 (1–2)*, 77–92. DOI: https://doi.org/10.1016/j.memsci.2007.07.032

[90] D. Sanz-Villanueva, D. Alique, A. J. Vizcaíno, J. A. Calles, R. Sanz, On the long-term stability of Pd-membranes with TiO_2 intermediate layers for H_2 purification, *Int. J. Hydrogen Energy* **2022**, *47 (21)*, 11402–11416. DOI: https://doi.org/10.1016/j.ijhydene.2021.12.005

[91] D. J. Rivera, C. L. Muhich, Preventing H_2S poisoning of dense Pd membranes for H_2 purification using an electric-field: An Ab initio study, *Surf. Sci.* **2023**, *733*, 122303. DOI: https://doi.org/10.1016/j.susc.2023.122303

[92] R. Ben-Mansour, M. A. Haque, M. A. Habib, S. Paglieri, A. Harale, E. M. A. Mokheimer, Effect of temperature and heat flux boundary conditions on hydrogen production in membrane-integrated steam-methane reformer, *Appl. Energy* **2023**, *346*, 121407. DOI: https://doi.org/10.1016/j.apenergy.2023.121407

[93] A. Iulianelli, G. Manzolini, M. D. Falco, S. Campanari, T. Longo, S. Liguori, A. Basile, H_2 production by low pressure methane steam reforming in a Pd-Ag membrane reactor over a Ni-based catalyst: Experimental and modeling, *Int. J. Hydrogen Energy* **2010**, *35 (20)*, 11514–11524. DOI: https://doi.org/10.1016/j.ijhydene.2010.06.049

[94] H. Lee, B. Lee, M. Byun, H. Lim, Comparative techno-economic analysis for steam methane reforming in a sorption-enhanced membrane reactor: Simultaneous H_2 production and CO_2 capture, *Chem. Eng. Res. Des.* **2021**, *171*, 383–394. DOI: https://doi.org/10.1016/j.cherd.2021.05.013

[95] A. Tran, A. Aguirre, M. Crose, H. Durand, P. D. Christofides, Temperature balancing in steam methane reforming furnace via an integrated CFD/data-based optimization approach. *Comput. Chem. Eng.* **2017**, *104*, 185–200. DOI: https://doi.org/10.1016/j.compchemeng.2017.04.013

[96] L. Xie, M. A. Lundteigen, Y.-L. Liu, Performance analysis of safety instrumented systems against cascading failures during prolonged demands, *Reliab. Eng. Syst. Saf.* **2021**, *216*, 107975. DOI: https://doi.org/10.1016/j.ress.2021.107975

[97] I. H. Moskowitz, W. D. Seider, M. Soroush, U. G. Oktem, J. E. Arbogast, Chemical process simulation for dynamic risk analysis: A steam-methane reformer case study, *Ind. Eng. Chem. Res.* **2015**, *54 (16)*, 4347–4359. DOI: https://doi.org/10.1021/ie5038769

[98] A.-B. Zhang, A. Barros, Y.-L. Liu, Performance analysis of redundant safety-instrumented systems subject to degrada-

21969744, 0, Downloaded from https://onlinelibrary.wiley.com/doi/10.1002/cben.202300049 by China University Of Mining, Wiley Online Library on [31/01/2024]. See the Terms and Conditions (https://onlinelibrary.wiley.com/terms-and-conditions) on Wiley Online Library for rules of use; OA articles are governed by the applicable Creative Commons License

tion and external demands, *J. Loss Prev. Process Ind.* **2019**, *62*, 103946. DOI: https://doi.org/10.1016/j.jlp.2019.103946
[99] W.-T. He, X.-Y. Wang, K. Qiu, J. Zhu, W.-J. Huang, Architecture design and safety research of a double-triple-channel redundant and fault-tolerant system, *J. Loss Prev. Process Ind.* **2016**, *44*, 495–502. DOI: https://doi.org/10.1016/j.jlp.2016.07.029
[100] J. Dugué, Fired equipment safety in the oil & gas industry: A review of changes in practices over the last 50 years, *Energy Procedia* **2017**, *120*, 2–19. DOI: https://doi.org/10.1016/j.egypro.2017.07.151
[101] F.-J. Deng, F. Wang, Misoperation monitoring and early warning during startup and shutdown of petrochemical units, *J. Loss Prev. Process Ind.* **2020**, *67*, 104265. DOI: https://doi.org/10.1016/j.jlp.2020.104265
[102] M. Attarian, A. K. Taheri, S. Jalilvand, A. Habibi, Microstructural and failure analysis of welded primary reformer furnace tube made of HP-Nb micro alloyed heat resistant steel, *Eng. Failure Anal.* **2016**, *68*, 32–51. DOI: https://doi.org/10.1016/j.engfailanal.2016.05.023
[103] S. Zheng, Y. Qin, W.-C. Li, F.-F. Huang, Y.-J. Qiang, S.-W. Yang, L. Wen, Y. Jin, Effect of hydrogen traps on hydrogen permeation in X80 pipeline steel – a joint experimental and modelling study, *Int. J. Hydrogen Energy* **2023**, *48 (12)*, 4773–4788. DOI: https://doi.org/10.1016/j.ijhydene.2022.10.038
[104] Y.-J. Li, Z.-R. Wang, X.-M. Shi, R.-J. Fan, Safety analysis of hydrogen leakage accident with a mobile hydrogen refueling station, *Process Saf. Environ. Prot.* **2023**, *171*, 619–629. DOI: https://doi.org/10.1016/j.psep.2023.01.051
[105] H. Li, X.-W. Cao, H.-M. Du, L. Teng, Y.-B. Shao, J. Bian, Numerical simulation of leakage and diffusion distribution of natural gas and hydrogen mixtures in a closed container, *Int. J. Hydrogen Energy* **2022**, *47 (84)*, 35928–35939. DOI: https://doi.org/10.1016/j.ijhydene.2022.08.142
[106] H. Böttler, X. Chen, S. Xie, A. Scholtissek, Z. Chen, C. Hasse, Flamelet modeling of forced ignition and flame propagation in hydrogen-air mixtures, *Combust. Flame* **2022**, *243*, 112125. DOI: https://doi.org/10.1016/j.combustflame.2022.112125
[107] M. H. S. Saeid, J. Khadem, S. Emami, M. Ghodrat, Effect of diffusion time on the mechanism of deflagration to detonation transition in an inhomogeneous mixture of hydrogen-air, *Int. J. Hydrogen Energy* **2022**, *47 (55)*, 23411–23426. DOI: https://doi.org/10.1016/j.ijhydene.2022.05.116
[108] Y.-F. Zhang, A. Musa, Influence of coaxial air jet on mass diffusion of hydrogen jet injected through lobe-injector at supersonic flow, *Int. J. Hydrogen Energy* **2022**, *47 (84)*, 35886–35896. DOI: https://doi.org/10.1016/j.ijhydene.2022.08.140
[109] H. Li, X.-W. Cao, Y. Liu, Y.-B. Shao, Z.-L. Nan, L. Teng, W.-S. Peng, J. Bian, Safety of hydrogen storage and transportation: An overview on mechanisms, techniques, and challenges, *Energy Rep.* **2022**, *8*, 6258–6269. DOI: https://doi.org/10.1016/j.egyr.2022.04.067
[110] E. Abohamzeh, F. Salehi, M. Sheikholeslami, R. Abbassi, F. Khan, Review of hydrogen safety during storage, transmission, and applications processes, *J. Loss Prev. Process Ind.* **2021**, *72*, 104569. DOI: https://doi.org/10.1016/j.jlp.2021.104569
[111] X.-L. Sun, L.-F. Hao, L.-Y. Chen, X.-K. Guo, C. Han, J.-F. Chen, W.-C. Jiao, R.-G. Wang, X.-D. He, Spray deposition of colorimetric H_2 detector with Pd/MoO_3 nanocomposites for rapid hydrogen leakage monitoring at room temperature, *Appl. Surf. Sci.* **2022**, *599*, 153878. DOI: https://doi.org/10.1016/j.apsusc.2022.153878
[112] S. T. Le, T. N. Nguyen, S. Linforth, T. D. Ngo, Safety investigation of hydrogen energy storage systems using quantitative risk assessment, *Int. J. Hydrogen Energy* **2023**, *48 (7)*, 2861–2875. DOI: https://doi.org/10.1016/j.ijhydene.2022.10.082
[113] K. Liu, C.-X. He, Y.-Z. Yu, C.-Y. Guo, S.-M. Lin, J.-Y. Jiang, A study of hydrogen leak and explosion in different regions of a hydrogen refueling station, *Int. J. Hydrogen Energy* **2023**, *48 (37)*, 14112–14126. DOI: https://doi.org/10.1016/j.ijhydene.2022.12.267
[114] P. Xu, J.-Y. Zheng, P.-F. Liu, R. Chen, F.-M. Kai, L. Li, Risk identification and control of stationary high-pressure hydrogen storage vessels, *J. Loss Prev. Process Ind.* **2009**, *22 (6)*, 950–953. DOI: https://doi.org/10.1016/j.jlp.2008.08.008
[115] S. Shang, J. Zhang, J.-X. Zhang, T.-P. Luo, M.-S. Bi, H.-P. Jiang, Y.-C. Li, W. Gao, Study on the effect of explosion suppression equipment on hydrogen explosions, *J. Loss Prev. Process Ind.* **2023**, *83*, 105046. DOI: https://doi.org/10.1016/j.jlp.2023.105046
[116] F.-Y. Long, Y.-L. Duan, S.-W. Yu, H.-L. Jia, Y.-B. Bu, J. Huang, Effect of porous materials on explosion characteristics of low ratio hydrogen/methane mixture in barrier tube, *J. Loss Prev. Process Ind.* **2022**, *80*, 104875. DOI: https://doi.org/10.1016/j.jlp.2022.104875
[117] Q.-X. Gao, X.-H. Qu, W. Peng, P. Zhang, S.-Z. Chen, Influence of obstacle morphology on safety of nuclear hydrogen production system, *Int. J. Hydrogen Energy* **2022**, *47 (86)*, 36733–36748. DOI: https://doi.org/10.1016/j.ijhydene.2022.08.235
[118] Y. Wu, X. Yu, Z.-C. Wang, H. Jin, Y.-Q. Zhao, C.-J. Wang, Z.-H. Shen, Y. Liu, W. Wang, The flame mitigation effect of N_2 and CO_2 on the hydrogen jet fire, *Process Saf. Environ. Prot.* **2022**, *165*, 658–670. DOI: https://doi.org/10.1016/j.psep.2022.07.027
[119] J.-Y. Wang, Y.-T. Liang, Z.-Z. Zhao, Effect of N_2 and CO_2 on explosion behavior of H_2-liquefied petroleum gas-air mixtures in a confined space, *Int. J. Hydrogen Energy* **2022**, *47 (56)*, 23887–23897. DOI: https://doi.org/10.1016/j.ijhydene.2022.05.152
[120] K. Chau, A. Djire, F. Khan, Review and analysis of the hydrogen production technologies from a safety perspective, *Int. J. Hydrogen Energy* **2022**, *47 (29)*, 13990–14007. DOI: https://doi.org/10.1016/j.ijhydene.2022.02.127
[121] I. A. Altuwair, F. Khan, Safety analysis of instantaneous release of compressed natural gas from a cylinder, *J. Loss Prev. Process Ind.* **2020**, *68*, 104284. DOI: https://doi.org/10.1016/j.jlp.2020.104284
[122] F. Alrashed, U. Zahid, Comparative analysis of conventional steam methane reforming and PdAu membrane reactor for the hydrogen production, *Comput. Chem. Eng.* **2021**, *154*, 107497. DOI: https://doi.org/10.1016/j.compchemeng.2021.107497

21969744, 0, Downloaded from https://onlinelibrary.wiley.com/doi/10.1002/cben.202300049 by China University Of Mining, Wiley Online Library on [31/01/2024]. See the Terms and Conditions (https://onlinelibrary.wiley.com/terms-and-conditions) on Wiley Online Library for rules of use; OA articles are governed by the applicable Creative Commons License

[123] S. Foresti, G. D. Marcoberardino, G. Manzolini, N. D. Nooijer, F. Gallucci, M. v. S. Annaland, A comprehensive model of a fluidized bed membrane reactor for small-scale hydrogen production, *Chem. Eng. Process.* **2018**, *127*, 136–144. DOI: https://doi.org/10.1016/j.cep.2018.01.018

[124] A.-B. Zhang, T.-L. Zhang, A. Barros, Y.-L. Liu, Optimization of maintenances following proof tests for the final element of a safety-instrumented system, *Reliab. Eng. Syst. Saf.* **2020**, *196*, 106779. DOI: https://doi.org/10.1016/j.ress.2019.106779

[125] J. Ji, Q. Tong, F. Khan, M. Dadashzadeh, R. Abbassi, Risk-based domino effect analysis for fire and explosion accidents considering uncertainty in processing facilities, *Ind. Eng. Chem. Res.* **2018**, *57 (11)*, 3990–4006. DOI: https://doi.org/10.1021/acs.iecr.8b00103

21969744, 0, Downloaded from https://onlinelibrary.wiley.com/doi/10.1002/cben.202300049 by China University Of Mining, Wiley Online Library on [31/01/2024]. See the Terms and Conditions (https://onlinelibrary.wiley.com/terms-and-conditions) on Wiley Online Library for rules of use; OA articles are governed by the applicable Creative Commons License

Hydrogen production by steam methane reforming and its risk factors are evaluated. The safety requirements for key device and materials as well as the safety optimization methods for each process and response measures for typical accidents are assessed and discussed. Future research demands are proposed from the perspective of research and development, being essential for improving safety.

Risk Identification and Safety Technology for Hydrogen Production from Natural Gas Reforming

Lele Feng, Yifan Gu, Jiabao Pang, Liangliang Jiang*, Jie Liu, Hang Zhou*, Biao Wang, Saeideh Babaee

ChemBioEng Rev. **2024**, *11 (X)*, **XXX ··· XXX**

DOI: 10.1002/cben.202300049

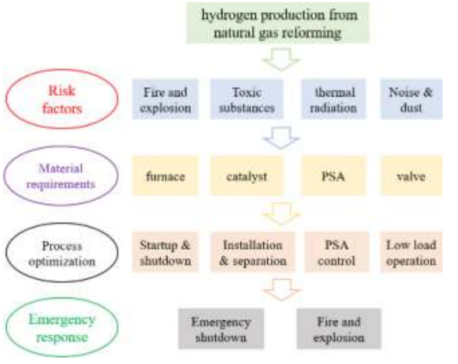

 © 2024 Wiley-VCH GmbH

21969744, 0, Downloaded from https://onlinelibrary.wiley.com/doi/10.1002/cben.202300049 by China University Of Mining, Wiley Online Library on [31/01/2024]. See the Terms and Conditions (https://onlinelibrary.wiley.com/terms-and-conditions) on Wiley Online Library for rules of use; OA articles are governed by the applicable Creative Commons License